Similarly, let us think of the number of vapor recompression schemes for distillation columns that have been considered in the past without knowledge of the pinch phenomenon. The appropriate placement concept shows that these schemes can never have a chance of producing net energy savings (compared to a properly integrated process), if the distillation column reboiler and condenser lie on the same side of the pinch. Also, for technical and economic reasons concerned with the heat pumping equipment itself, the temperature difference between boiler and condenser needs to be small. And even if these two criteria are met, the "need" for vapor recompression can be designed out of the system by altering column pressure appropriately, so as to eliminate the problem at source (Dunford and Linnhoff, 1981). Hence, future possibilities for vapor recompression viable in otherwise well-integrated processes seem to be rare.

ACKNOWLEDGMENT

The authors acknowledge the many contributions of all members of the Process Synthesis Team in the ICI New Science Group, and thank ICI Ltd. for permission to publish the paper.

NOTATION

CP = heat capacity-flowrate, MW/°C
F = heat flow, MW
ΔH = difference of enthalpy flow, MW
$\Sigma_j(\Delta H)_j$ = enthalpy balance over all streams j, MW
$\Sigma_i\Sigma_j(\Delta H)_{i,j}$ = enthalpy balance over all temperature intervals i of all streams j existing within intervals i, MW
Q = heat quantity or flow, MJ or MW
Q_{IN} = minimum hot utility requirement for heat recovery problem, MW
Q_{OUT} = minimum cold utility requirement for heat recovery problem, MW
T = temperature, K
T_b = interval boundary temperature, °C
ΔT = temperature difference, °C
ΔT_{min} = minimum approach temperature difference, °C
W = Work or power, MJ or MW
α = heat engine or heat pump temperature efficiency, dimensionless
η = total heat engine or heat pump efficiency, dimensionless
η_E = heat engine or heat pump machine efficiency, dimensionless

LITERATURE CITED

Dunford, H. A., and B. Linnhoff, "Energy Savings by Appropriate Integration of Distillation Columns into Overall Processes," Paper No. 10, Symp. on "Cost Savings in Distillation," Leeds (1981).

Linnhoff, B., and J. R. Flower, "Synthesis of Heat Exchanger Networks." *AIChE J.* **24**, 633 (1978).

Linnhoff B., D. R. Mason, and I. Wardle, "Understanding Heat Exchanger Networks," *Comp. and Chem. Eng.*, **3**, 295 (1979).

Linnhoff, B., and J. A. Turner, "Heat Exchanger Network Design: New Insights Give Big Savings," *Chem. Eng.*, 56 (Nov. 1981).

Menzies, M. A., and A. I. Johnson, "Synthesis of Optimal Energy Recovery Networks Using Discrete Methods," *Can. J. of Chem. Eng.*, **11**, 271 (1972).

Nishida, N., G. Stephanopoulos, and A. W. Westerberg, "A Review of Process Synthesis," *AIChE J*, **27**(3) 321 (1981).

Nishio, M., J. Itoh, K. Shiroko, and T. Umeda, "Thermodynamic Approach to Steam-Power System Design," *Ind. Eng. Chem. Process Des. Dev.*, **19**, 306 (1980).

Umeda, T., F. Itoh, and K. Shiroko, "Heat Exchange System Synthesis," *Chem. Eng. Prog.*, 70 (July, 1978).

Whistler, A. M., "Heat Exchangers as Money Makers," *Pet. Refiner*, **27**, 83 (1948).

Manuscript received February 25, 1982; revision received October 5, and accepted October 20, 1982.

Part II: Design Procedure for Equipment Selection and Process Matching

In Part I, criteria for heat engine and heat pump placement in chemical process networks were derived, based on the "temperature interval" (T.I) analysis of the heat exchanger network problem. Using these criteria, this paper gives a method for identifying the best outline design for any combined system of chemical process, heat engines, and heat pumps. The method eliminates inferior alternatives early, and positively leads on to the most appropriate solution. A graphical procedure based on the T.I. analysis forms the heart of the approach, and the calculations involved are simple enough to be carried out on, say, a programmable calculator. Application to a case study is demonstrated.

Optimization methods based on this procedure are currently under research.

D. W. TOWNSEND

ICI New Science Group
Runcorn, Cheshire, England

BODO LINNHOFF

University of Manchester Institute of Science and Technology (UMIST)
Manchester M60 1QD, England

SCOPE

In part I, it was shown that from an understanding of the "pinch" phenomenon in heat recovery networks, the concepts of "appropriate" and "inappropriate" placement for heat engines and heat pumps follow. Appropriate placement of heat engines in integrated process networks makes it possible to produce work from heat at 100% efficiency. Inappropriate placement cannot give efficiencies greater than "stand-alone." Conversely for heat pumps, stand-alone efficiency can be achieved only by appropriate placement, and inappropriate placement is fundamentally wasteful.

Following these discoveries, this paper shows that it is possible to identify a "thermodynamic best" appropriately-placed heat engine or heat pump device in any given heat recovery network. With an appropriately-placed "thermodynamic best" heat engine, work output at 100% efficiency is maximized. However, this engine would involve impractical complexity, both in the heat exchanger network and in the engine cycle design. A method for determining the "best practical" config-

Correspondence concerning this paper should be addressed to D. W. Townsend.

uration is presented which involves finding the best compromise between energy efficiency and complexity of design. It uses as a basis the "process source/sink profile" derived from the Temperature Interval (T.I.) analysis of the heat exchanger network problem.

The paper considers explicitly the use of steam Rankine cycles, gas turbine cycles, and organic fluid Rankine cycles, in the light of the procedure. Heat pumps, and other heat and power devices are not discussed explicitly but all procedures would be entirely analogous. The paper demonstrates the procedure in application to a case study, where the "state-of-the-art" design is shown to pay a 40% net energy penalty when compared with the "best practical" design as identified using the new method.

CONCLUSIONS AND SIGNIFICANCE

Following from the understanding of appropriate heat engine and heat pump placement described in Part I, this paper introduces the use of the "process source/sink profile" and provides a simply-applied design procedure for selection of the best practical power technology in any given design context. The procedure is based on fundamental principles derived from thermodynamic analysis. Thus it can always form a point of reference and take account of practical design constraints. The procedure can be used to evaluate options at the preliminary design stage and to identify the preferred configuration for chemical and other processes involving integrated heat recovery and power generation.

The procedure represents a breakthrough in the general area of process synthesis as it is the first procedure published for heat and power integration that takes into account the fundamental importance of the heat recovery pinch.

PROCESS SOURCE/SINK PROFILE

The "process source/sink profile" forms the basis of the procedure. It is described first for the assumption of "thermodynamic best" fits between process and heat engine. Then, cases involving practical tradeoffs are discussed.

Heat Engines in the *T-H* Diagram

All heat engines and heat pumps employ a working fluid to effect the heat and work transformation. That is to say, via heat exchangers (which may be direct contact or indirect), the working fluid in an engine absorbs heat from an external source, passes through the mechanical devices which effect the transformation from heat to work and rejects heat to a sink. These heat-absorbing and rejecting parts of the cycle can be represented on *T-H* diagrams; i.e., they can be handled by the T.I. analysis. Figures 1(a) and (b) represent idealized systems, in which heat engines operate between heat source σ_1 and heat sink σ_2. In Figure 1(a), the heat engine employs a working fluid whose *T-H* profiles run parallel to those of the source and sink streams. Thus, the minimum allowable temperature difference exists throughout the heat-absorbing and rejecting heat exchangers. In Figure 1(b), the working fluid undergoes latent heat changes, and the minimum temperature difference occurs at only one point in the heat exchangers. Remembering, from Part I (Eq. 4) that

$$W = \eta_E . \alpha . Q$$

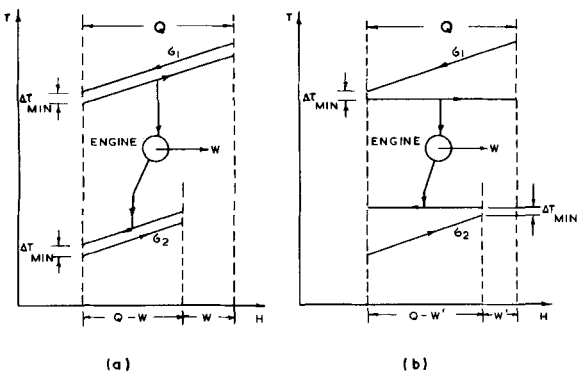

Figure 1. Heat engines, T-H representation.

it is clear that η_E is greater in Figure 1(a) than in Figure 1(b), because the wasted driving force in the heat exchangers is smaller. It should be noted that in Figure 1(b), even if the exchangers had infinite surface area, η_E could never become unity. This is not true, however, of Figure 1(a). By virtue of the fact that "parallel profiles" have been chosen, no driving force is wasted at all. So there is an energy incentive for arranging for profiles which approach the parallel case.

Process Profile, and Profile Matching

Consider a heat engine placed entirely above the pinch, such that the heat recovery network receives heat from the engine exhaust instead of directly from hot utility. As described in Part I, such placement allows work generation at 100% efficiency. Maximizing the work output means minimizing the driving force losses. Hence, there must be minimal temperature differences between the heat engine working fluid and the process. In other words, the profile of the engine exhaust stream in the *T-H* diagram, when included in the heat recovery problem, must reduce all temperature differences above the pinch to minimum, analogous to the case in Figure 1(a). This will be further considered shortly.

Figure 2(a) shows the "cascade diagram" for the example problem introduced in Part I (Part I, Figure 3). Figure 2(b) shows the process heat flows plotted against interval boundary temperatures. The arrow heads on the plot show whether a section of the plot represents a heat source or a heat sink. Where the heat flow increases at increasing temperature, the process is a heat sink. Conversely, increasing heat flow at decreasing temperature means that, in that region, the process is a heat source. The pinch appears as the point of gradient change at zero flow.

We now realize that although the graph has been constructed by plotting heat flows, it does represent the net temperature-enthalpy characteristic of the total process. This is because the Problem Table Algorithm derives the heat flows from a cumulative summation of all the individual interval enthalpy balances. Thus we can legitimately change the energy axis from "Heat Flow" to "*H*," as done in Figures 2(c) and (d).

Note that the source parts of the process source/sink profile are not consistent in their gradient in the *T-H* diagram with the convention normally adopted. The direction is reversed. However, the representation shown in Figure 2(b) is convenient because it is derived directly from the heat flow figures in the Problem Table, and because it clearly shows the location of the pinch.

If we define an engine exhaust stream whose *T-H* profile lies

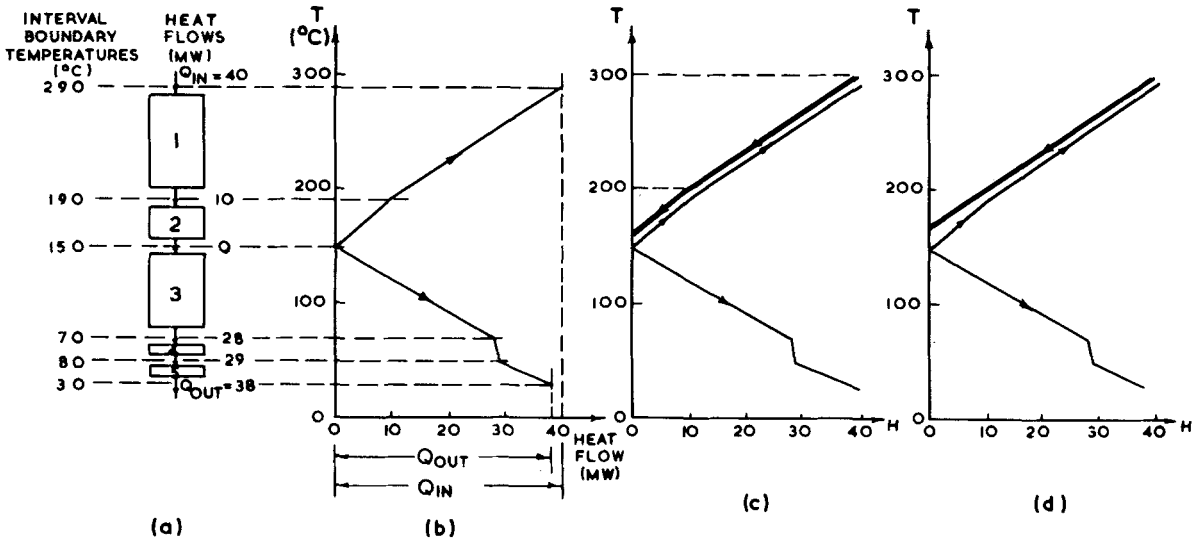

Figure 2. Construction of heat engine exhaust profiles above the pinch, using example problem.

all above the process sink profile (i.e., the process profile above the pinch), it will be capable of supplying all necessary process heating. If we then construct such a stream profile running countercurrent to the process sink profile and everywhere $\frac{1}{2}\Delta T_{min}$ above it, we will fulfill the criterion stated above for maximum work output. Namely, such an exhaust stream will everywhere exactly match the net process stream profile in each temperature interval, maintaining the global ΔT_{min} requirement for matches between exhaust and process. So, remembering that $\Delta T_{min} = 20°C$, in interval 1 such an exhaust stream must have a total heat content of 30 MW and run from 300 to 200°C. Similarly, in interval 2 the exhaust stream must have a total heat content of 10 MW and run from 200 to 160°C. This profile is plotted in heavy line above the process sink profile in Figure 2(c). Note that the total heat content of the exhaust stream is equal to the total process heat requirement (i.e., 40 MW).

Loss of Driving Force in Simpler Engines

Constructing parallel profiles in the way described above, defines the "thermodynamic best" heat engine, i.e., the one that maximizes work output because degradation of driving forces is minimized. However, the exercise will probably not define the best practical system because an impractically complex heat recovery network will be required. Also, each discrete change in the exhaust flowrate predicted implies a separate power cycle (two cycles are implied in the example above), which again might mean impractical complexity. However, the process source/sink profile forms a good basis for the preliminary definition of practical systems. Simplification can be achieved by reducing the number of power cycles. So for example in the problem shown in Figure 2, the two-cycle minimum driving force solution can be approximated by a single-cycle solution, Figure 2(d), with little loss of work output: the departure from minimum driving forces is small. More discussion on the definition of practical systems is given later.

Reconstructing Problem Table

Having used the process sink profile to predict a candidate engine exhaust profile, the Problem Table can then be reconstructed to include the exhaust stream. The exhaust profile shown in Figure 2(d) has a CP of 0.3 MW/°C and a total heat content of 40 MW (i.e., after the simplification it still covers the whole process heat requirement). This means that it runs from 300 to 166.7°C. The Problem Table for the modified heat recovery problem is shown in Figure 3(a), with the exhaust stream labelled "5" (Part I, Figure 3(a) for the original Problem Table). The temperature intervals are labelled to correspond to the cascade diagram shown in Figure 2(a). Because the engine exhaust stream does not extend as far as 160°C, interval number 2 is now split into two. As expected, the Problem Table predicts that no external heating is required (a zero at the top of column 4) and that the total cooling duty is unchanged (38 MW indicated at the bottom of column 5). Comparing the original cascade diagram, Figure 2(a), with the modified diagram, Figure 3(b), the position of the original process pinch is unchanged, but above this pinch the addition of the exhaust stream has created a new pinch extending throughout interval number 1 (input and output heat flows both zero). The small heat flow in interval number 2 confirms the presence of a small excess driving force in this region. (Compare Figure 2(d).)

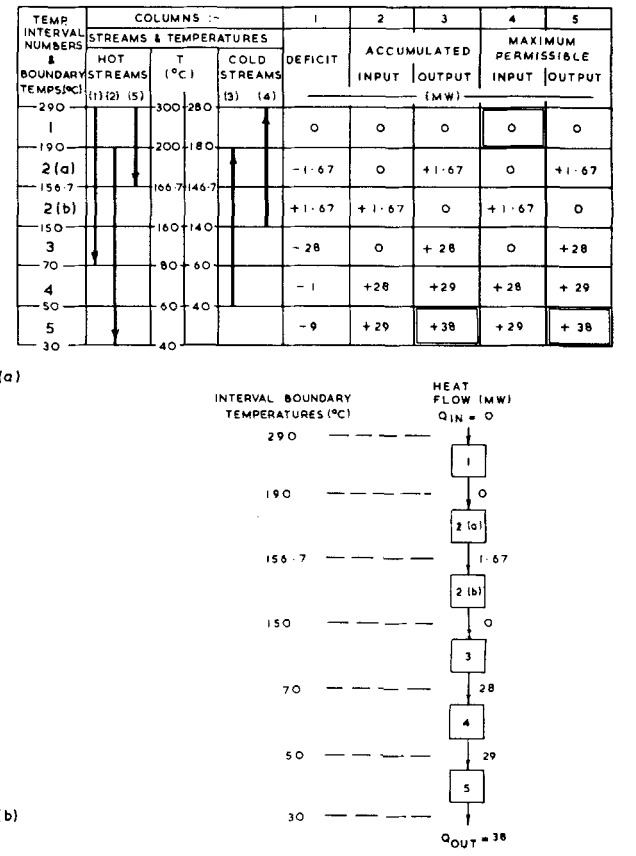

Figure 3. Temperature interval analysis for example problem with engine exhaust added above the pinch.

Having reconstructed the Problem Table, explicit design methods can be used to design the heat recovery network, as described for example, by Linnhoff and Hindmarsh (1983).

ΔT_{min} Contributions

Throughout the preceding example it was assumed that all heat exchange matches, process-to-process and engine-to-process, were subject to a ΔT_{min} of 20°C. Usually in industrial problems, the use of a global ΔT_{min} is not appropriate, and some match-dependence of ΔT_{min} is required. This can be introduced into the T.I. analysis method by assigning ΔT_{min} "contributions" to individual streams, as described in Part I. So for example, if gas streams are given a contribution of 20°C and liquid streams a contribution of 10°C, a gas/gas match will have a total ΔT_{min} of 40°C, a gas/liquid match a ΔT_{min} of 30°C, and a liquid/liquid match a ΔT_{min} of 20°C. Importantly in the present context, the engine or heat pump working fluid can be assigned an individual ΔT_{min} contribution. This is desirable because usually the criteria determining the process-to-process ΔT_{min} are different from those determining the engine working fluid-to-process ΔT_{min}. Note that streams can have negative contributions provided that this does not result in matches having a negative ΔT_{min}. The ability to assign ΔT_{min} contributions is exploited in the case study.

Heat Engines Below Pinch

Let us now consider a heat engine operating below the pinch. In this case, the engine heat absorption profile is fitted below the process source profile. The procedure is exactly analogous to the one described above. Again using the example problem, Figure 4 shows the shape of the heat absorption profile of a typical fluorocarbon Organic Rankine Cycle (O.R.C.) fitted underneath the process source profile. Note that here we have taken the simplification of the matching procedure a stage further.

In choosing a specific engine cycle, we are constraining the shape of the profile to be matched against the process. In this case, the match is not particularly good. The slope of the process source profile contrasts with the latent heat change in the O.R.C. boiler, which means that the match achieves minimum driving force at only one point. Substantial driving force losses exist elsewhere. Choosing a boiler temperature of 100°C, and assuming that R11 refrigerant is the working fluid, only about 22 MW of the total heat available of 38 MW can be absorbed by the O.R.C. The cycle technology thus constrains the power recovery to a quantity well

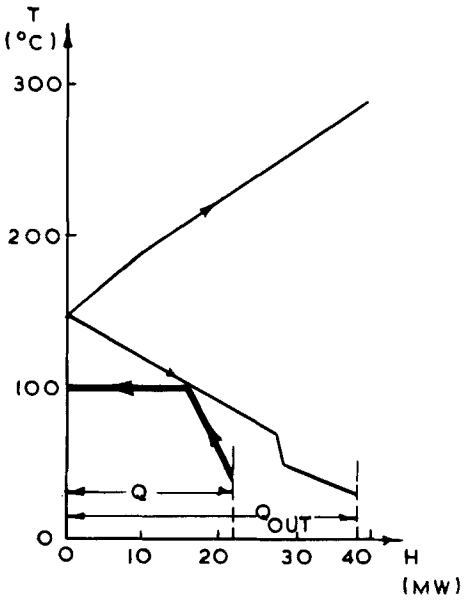

Figure 4. Construction of engine heat absorption profile below the pinch, using example problem.

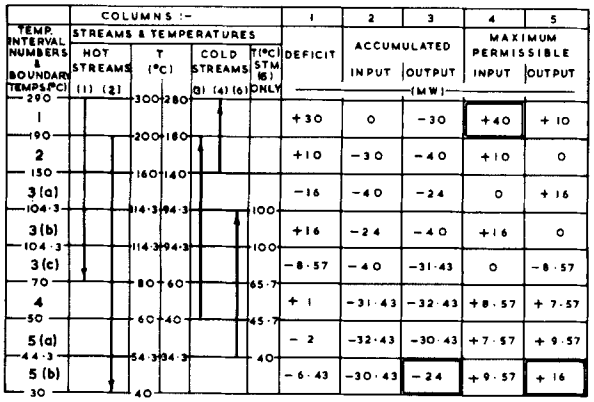

Figure 5. Temperature interval analysis for example problem with Rankine cycle heat absorption profile added below the pinch.

below the thermodynamic maximum. Such technological constraints will be discussed in general later.

Figure 5 shows the Problem Table for the total system of Figure 4. To handle the latent heat change of the O.R.C. absorption stream in the T.I. analysis, it is necessary to define two temperature interval boundaries at the same temperature, corresponding to the phase change temperature. To illustrate the handling of match-dependent ΔT_{min}, a ΔT_{min} contribution of 4.3°C is assigned to the O.R.C. stream. (This value is derived from the construction in Figure 4 where the boiler heat load is arbitrarily chosen as 16 MW at 100°C.) Thus ΔT_{min} in a match involving the working fluid is 14.3°C, whereas ΔT_{min} in any other match remains at 20°C. In Figure 5, the heat engine stream is labelled "6." In this case, integration of the heat engine means that the hot utility is unchanged. As predicted by construction in Figure 4, the cold utility is not reduced to zero, but only to 16 MW. This is the difference between the total heat available below the pinch (38 MW) and the heat absorbed by the O.R.C. (22 MW).

One, Two or More Cycles?

From here onwards, the discussion will be based for convenience on process source/sink profiles which are not related to numerical examples but chosen for qualitative illustration.

It has already been stated that to maximize work output at 100% efficiency, multiple engine cycles are required to reduce all driving forces to minimum. Also, in the example when fitting an engine exhaust profile above the pinch, it was shown how a single cycle could apporoximate closely the work output obtainable from the multiple (two)-cycle profile. In the general case, it is possible to identify by inspection best fit single cycles, double cycles, n–cycles,

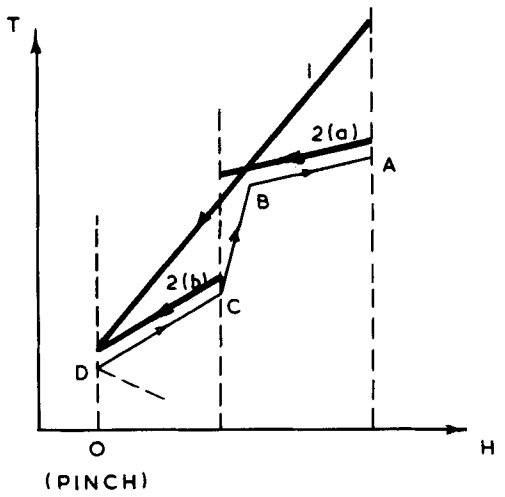

Figure 6. Single vs. multiple cycles.

etc. This allows quick evaluation of the potential benefit of additional cycles, Figure 6. Process sink profile DCBA above the pinch has the single-cycle profile 1 fitted against it, and a double-cycle profile 2(a) and (b). Profile 2(a) and (b) shows less loss of driving force against the sink than profile 1. One, therefore, expects profile 2 to show better energy performance, but at increased complexity and higher capital cost. Sensibly the process designer will evaluate the revenue from the marginal increase in work output from profile 2. He will also evaluate the increase in capital charges from cost estimates for the engine cycles and increased heat exchange surface area. Because he is dealing with a *discrete change*, rough cost estimates will usually be sufficient for identificatin of the better solution.

Reentrant Process Source/Sink Profiles

A pair of composite curves of the type shown in Figure 7(a) will yield a process source/sink profile as shown in Figure 7(b). In a heat recovery network, the heat from region AB in Figure 7(b) may be transferred anywhere into region DB at nonminimum temperature driving force. Similarly, heat from DE is transferred to FE. In the present context of heat and power integration, these temperature differences are perhaps exploitable.

In Figure 7(c), region AB (which is a "local" heat source existing above the pinch) is shown reversed into the normal source stream representation and shifted as far to the left as possible. This then represents the maximum temperature differences possible between AB and DB. In Figure 7(d), a heat engine is assumed to operate between the source AB and the process sink, with the exhaust heat supplying section DC′ of the sink. A second heat engine may then operate between the utility source and section C′B. The net work produced by the two engines is W'. Compare this system with that shown in Figure 7(e) where a single heat engine operates between the utility source and the net process sink DC (i.e., the sink remaining after the heat from AB has been transferred into CB), producing work W. Clearly, W' is greater than W because in Figure 7(d), all heat is transferred at minimum driving force. In general, wherever the process source/sink profile is "reentrant" (for example, points B and E in Figure 7(b)), potential could exist for gaining work at 100% efficiency by addition of "interprocess" heat engines.

The diagrams show idealized and therefore impractical cycles. The identification of real cycles follows the same logic as described before. That is to say, after fitting real cycles by inspection, marginal cost is traded against marginal benefit.

Where a single "local" source which exists above the pinch, such as AB in Figure 7(b), cannot be economically exploited by an additional engine cycle, it may be exploitable in conjunction with the utility source as shown in Figure 7(f). Whether or not such a single cycle yields a net power advantage over a single cycle matched as in Figure 7(e) will depend entirely on the source/sink loads and levels and the practical technology chosen. However, the designer should be aware of this option.

Notice that the profile shown in Figure 7(b) is a special case in that, effectively, it has two pinches (points D and F). [Note that point F is not a true pinch, but the point at which the composite curves are in enthalpy balance at the cold end—compare Figure 7(a).] Placing a heat engine between these points (i.e., operating over DEF) can still produce work at 100% efficiency. In the heat transfer problem, DE and FE are in heat load balance. Hence, when work is extracted it has to be made up from external heat to satisfy the heat balance of the process below the pinch. This can be done by cascading heat through the network, the heat flow at D becoming equal to the work produced. Alternatively, low-grade heat could be supplied over the relevant part of the temperature range EF. In both cases, the 100% efficiency claim remains valid.

Finally, consider the engine taking heat from source AB in Figure 7(d). It does not have to reject heat over DC′, but could reject it over any range within DB. However, rejecting heat at the low-temperature end of DB maximizes its efficiency and hence its work output. Of course, the engine operating from the utility source then has to reject its heat at the higher end of DB with reduced efficiency. In ideal cycles, the changes in work output between the engines exactly cancel out since the overall source and sink loads and levels are not changed. However, in a real system,

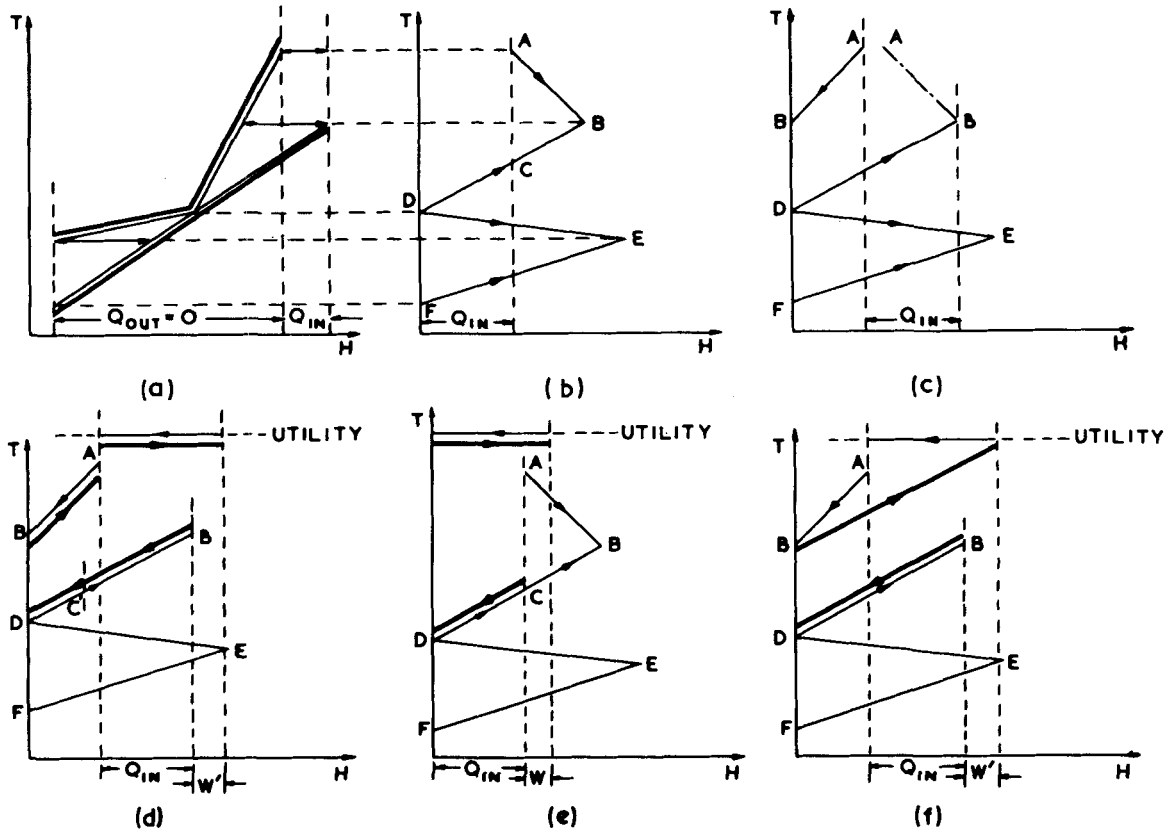

Figure 7. Exploiting temperature differences in reentrant process source/sink profiles.

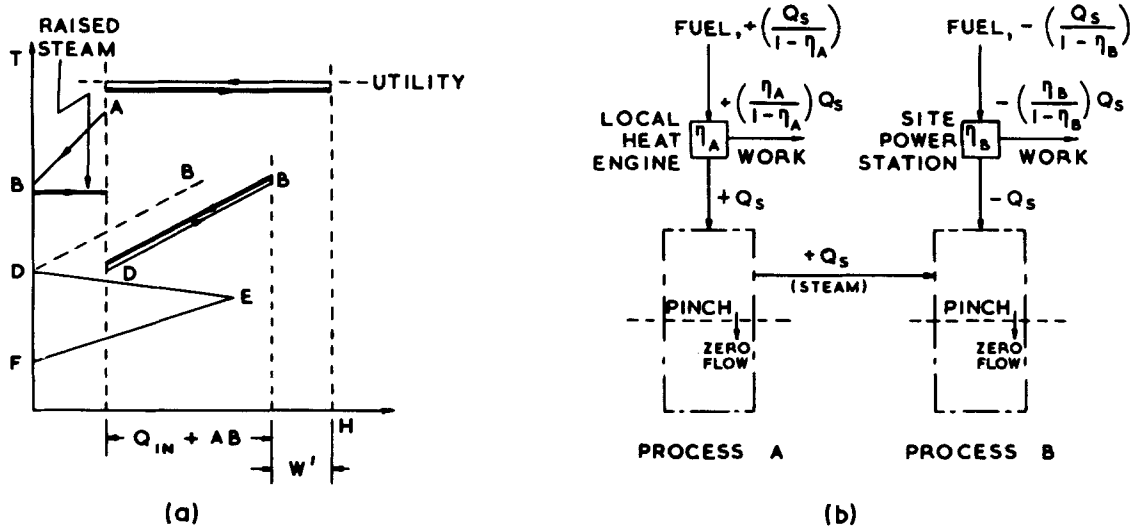

Figure 8. Effect of raising steam above the pinch.

the irreversibilities in engines operating across narrow source-to-sink temperature differences have a significant effect on engine efficiency. Thus in real systems it pays to examine the tradeoff between temperature-related engine-cycle efficiencies.

Raising Steam Above Pinch

Another way of exploiting the temperature differences in a process between reentrant parts of the process source/sink profile may present itself if the process is viewed in the context of an integrated site. For their contribution to the following observations, the authors are indebted to Stephanopoulos and Christodoulou (1982).

Although we would not usually consider raising steam above the pinch, let us examine what happens in the special case of simultaneous integration of a heat engine above the pinch and steam-raising above the pinch. If the process has a reentrant sink profile, Figure 7(b), we can use the "local" heat source AB not for matching against the heat input side of a heat engine but for raising steam for export from the plant. This then leaves a bigger net heat sink DB against which to match a heat engine, Figure 8(a). The result is more work produced at 100% efficiency than is possible in Figure 7(d).

However, we cannot conclude the analysis without considering the effect of the "export" steam on the site energy system. As shown in Figure 8(b), steam raised on plant A must replace utility steam supplied above the pinch on plant B. This replaced utility steam, on a large integrated site, will have come from the site power station. Thus the steam exported from plant A restricts the extent to which the site power station can produce work at nominally 100% efficiency, Figure 8(b). Simple algebra shows that, if the cycle efficiency of the heat engine on plant A is η_A and the power station cycle efficiency when integrated with plant B is η_B, with Q_S transferred as steam from A to B, the extra work produced at nominally 100% efficiency is:

$$\delta W' = Q_S \cdot \frac{(\eta_A - \eta_B)}{(1-\eta_A)(1-\eta_B)}$$

This can only be positive for $\eta_A > \eta_B$, i.e.; the local heat engine on plant A must have a larger cycle efficiency than the power station has when producing steam at the level as raised on plant A.

We conclude that this case is really analogous to those in Figures 7(d) and 7(f). The potential difference between AB and DB is being used only to increase 100% efficient work production, the *net* increase being the difference between W' in Figure 8(a) and the work production lost by the power station. Perhaps we should not really call this a special case. However, it is certainly a case that the designer should keep in mind since it might offer a more viable alternative than those illustrated in Figure 7.

Load vs. Level

In power systems, load and level interact. In heat engines the work value of a small quantity of heat at high level can be equivalent to that of a large quantity at low level. Similarly a large sink

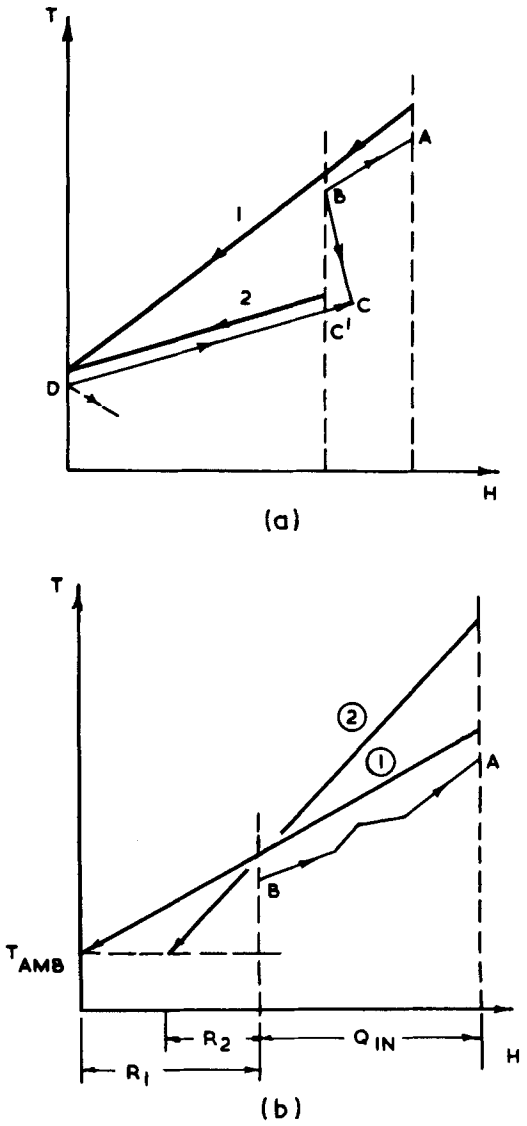

Figure 9. Load vs. level interaction.

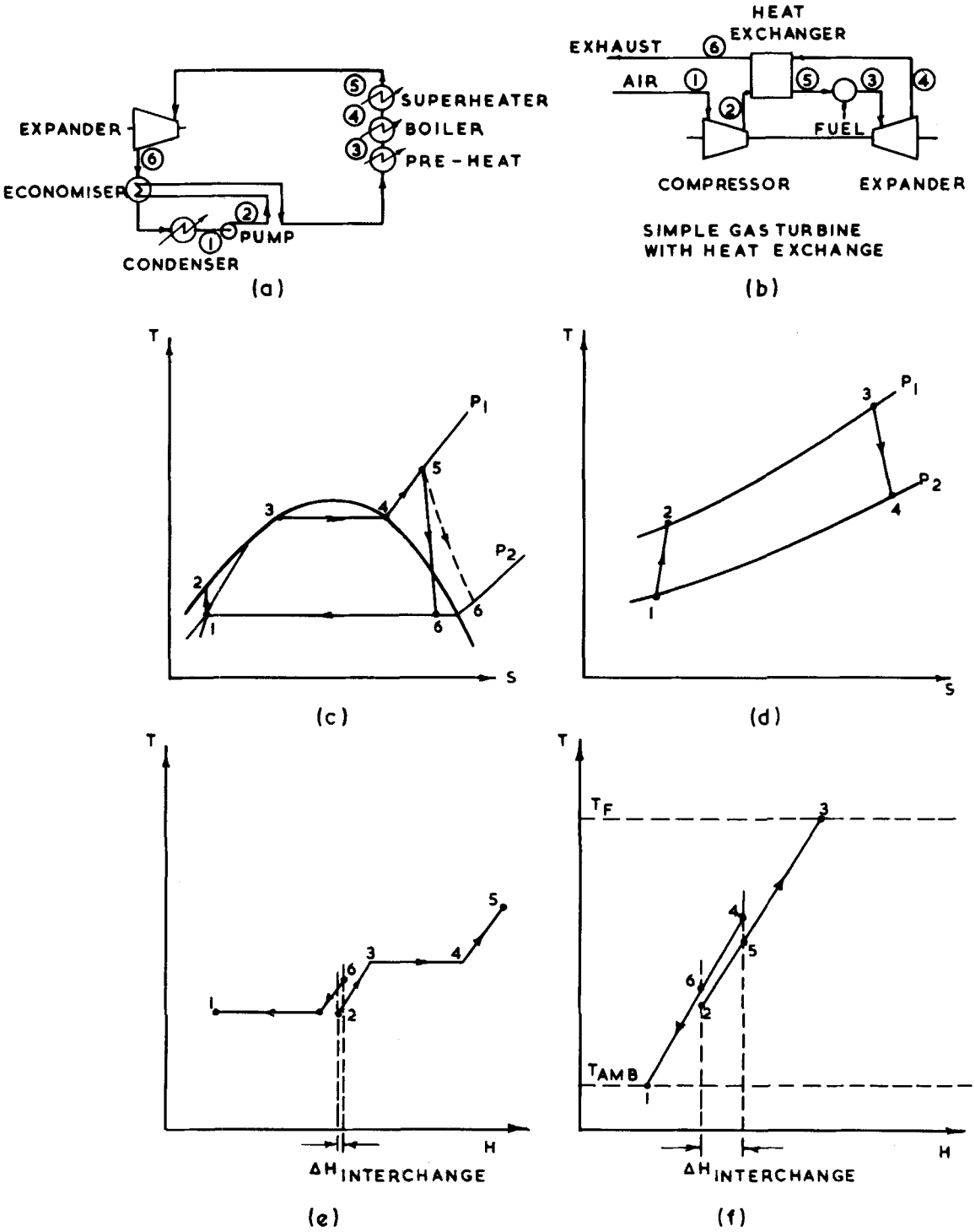

Figure 10. Rankine and open gas turbine cycles.

at high level can be equivalent to a small sink at low level. Figure 9(a) shows a process source/sink profile ABCD above the pinch. With this type of profile, an ambiguity based on loads and levels might exist for the integration problem. Engine exhaust profile 1 covers the whole heat sink with one cycle at rather higher level than profile 2. Profile 2 also consists of only one cycle but covers only part of the sink with better engine efficiency. Again, one should evaluate two discrete cases to find the better solution.

A similar ambiguity often arises with open heat engine cycles such as gas turbines. The lowest heat rejection temperature of these cycles is fixed at ambient. Therefore, in general, the designer is forced to reject some exhaust heat below the pinch, Figure 9(b). The process sink profile is BA. The process pinch lies at B and the process heat requirement is Q_{in}. Profiles 1 and 2 represent two choices of engine exhaust profile, with different heat rejection temperatures and different heat quantities R_1, R_2 rejected below the pinch. One must choose between them. Profile 1 rejects heat on average at a lower temperature, and will therefore give a better cycle efficiency than profile 2. However, the quantity of heat rejected to waste is greater for profile 1 than for profile 2. The situation is complicated by the fact that cycle efficiency above the pinch does not determine work generation efficiency but the amount of work obtainable at 100% efficiency (Part I). To determine the optimum profile, it is necessary to carry out an analysis of marginal benefits. Such an analysis forms part of the current research project in heat and power network design.

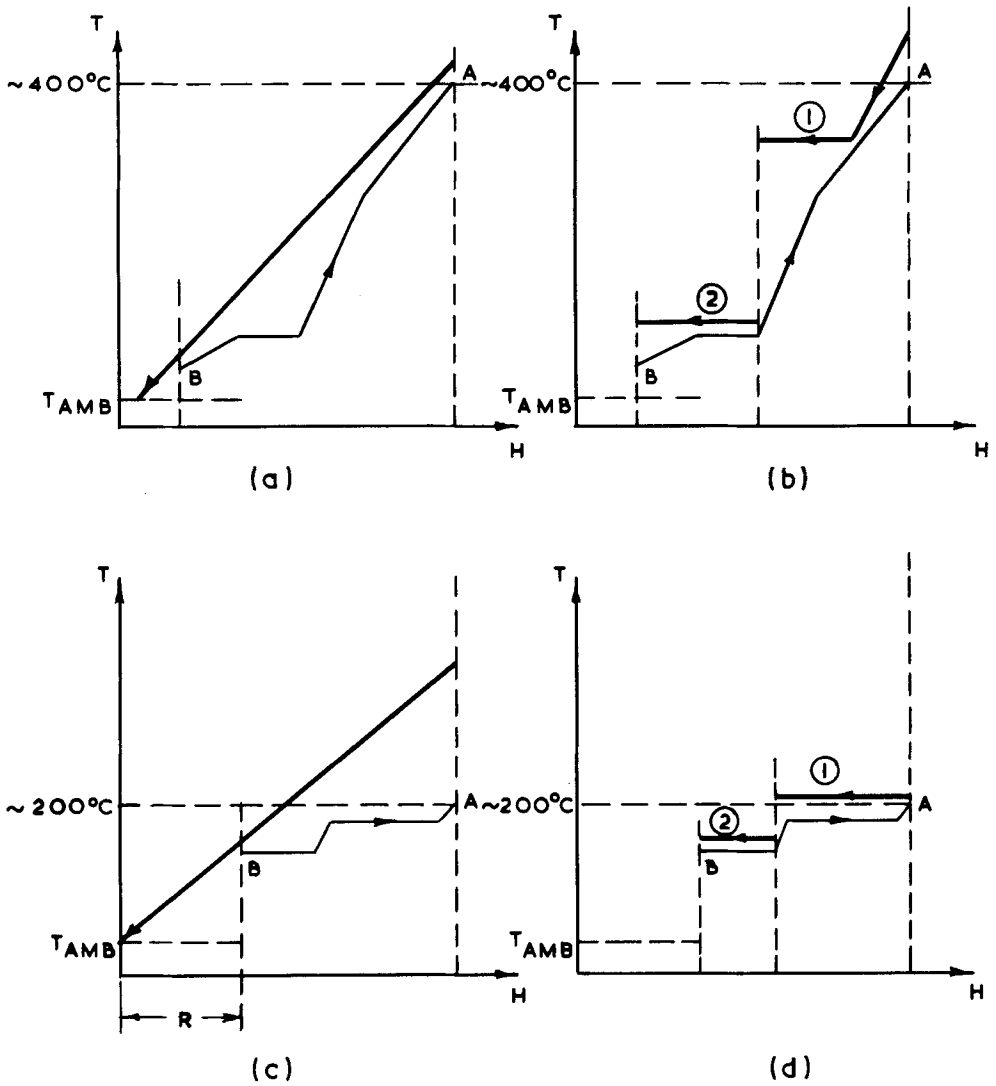

Figure 11. Technology selection with respect to process source/sink profile.

PRACTICAL HEAT ENGINES

So far in the discussion the characteristics of practical heat engines have only been touched on. However, some basic characteristics have to be considered now in the present context of integrated networks.

Engine Types and "External" Profiles

The large-scale "workhorses" of the chemical industry are steam turbine Rankine cycles and open-gas turbine (Joule-Brayton) cycles. Also important are closed-cycle gas turbines, organic Rankine cycles (for power recovery), and Diesels. Figures 10(a) and (b) show schematic diagrams of the Rankine cycle and gas turbine cycle, respectively. The relevant thermodynamic cycles are shown in Figures 10(c) and (d) in T-S diagrams, and the heat absorbing and heat rejecting profiles of the cycles are plotted on T-H coordinates in Figures 10(e) and (f). Based on the latter profiles, the concept of "external" engine profiles can be introduced. In the gas turbine case, Figure 10(f), part of the heating requirement 2–3 can be met by turbine exhaust 4–1, providing that $T_3 \geq T_2 + \Delta T_{min}$. (Compliance with this criterion and the amount of heat interchange possible depends mainly on the upper-cycle temperature T_3 and the pressure ratio p_1/p_2.) Thus the "external profiles," i.e., the heat rejection and absorption profiles relevant for the process integration, are given by 5–3 and 6–1. In the Rankine cycle case, Figure 10(e), the amount of interchange possible is very limited and only feasible when point 6 lies in the superheat region. The economizer-interchanger is, therefore, not normally employed in steam systems, although it is sometimes included in O.R.C. designs. However, if a steam Rankine cycle has multiple exhaust levels, high-level exhaust steam can be used to preheat low-level condensate.

Selecting Right Heat Engine

The process source/sink profile allows comparison of one heat engine type with another on the same process duty. In this connection, it is worth stating yet again an important conclusion reached in Part I. Namely, that when a heat engine is appropriately placed, the cycle efficiency affects the *quantity* of work available, but not the efficiency of work generation: appropriate placement always confers 100% efficiency. Figures 11(a) to (d) illustrate the relative performance of open-cycle gas turbines and steam turbine Rankine cycles on two different process source/sink profiles. In Figures 11(a) and (b), the "above the pinch" process sink profile BA extends from low to high temperature. This means that the gas turbine exhaust, Figure 11(a), is the most appropriate, with little energy wasted by rejection below the pinch, and a high efficiency for good work output in a single cycle.

Compare this with the steam turbine exhausts matched against the same process in Figure 11(b). Although work can be produced at 100% efficiency, driving force losses against the sink are large. This is true even if a back-pressure turbine having two (or more) exhaust levels is used, Figure 11(b). Also it should be remembered that in steam cycles, the indirect heat transfer from the heat source

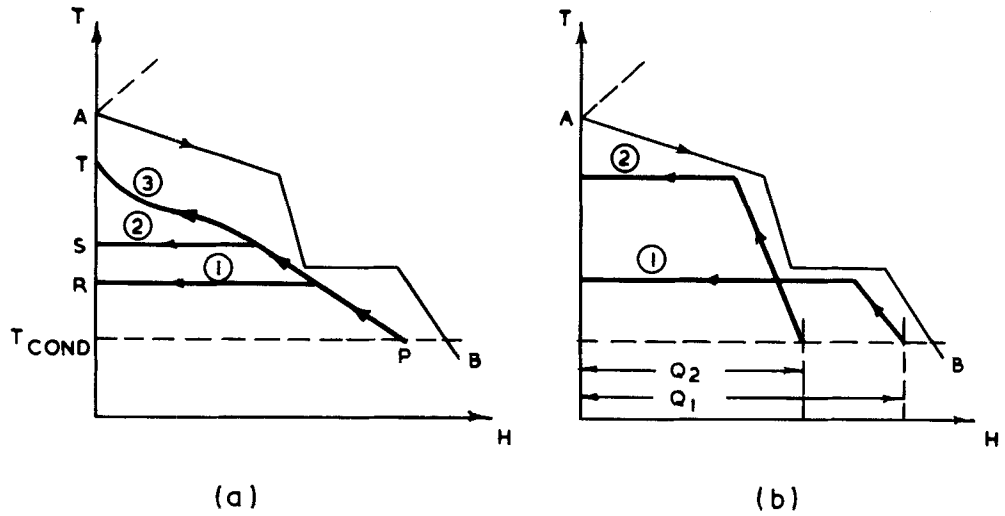

Figure 12. Rankine cycle power recovery, profile selection.

to the steam in the boiler/superheater means that the upper-cycle temperature is limited to a value much less than that achieved by a gas turbine. Hence driving force losses against the source are also higher. As a result, total work output is much smaller. Even if the work required by the process itself is small and the steam cycle can provide all of it, the gas turbine system represents an opportunity of producing power for "export" at a very high efficiency.

In Figures 11(c) and (d), the process sink profile BA exists at moderate temperature. This means that the steam Rankine cycle, Figure 11(d), can achieve better cycle efficiency and hence higher work output. On the other hand, the pinch exists at a temperature as high as possible in the context. The gas turbine, therefore, Figure 11(c), has to reject a significant quantity of heat below the pinch, and so much of the work output is achieved at no more than the cycle stand-alone efficiency.

Considering the fitting of Rankine cylces to process source profiles below the pinch, Figures 12(a) and (b) illustrate the principles involved. It should be noted that these principles have been discussed by other workers (for example, Sega, 1974; Ichikawa, 1970) in relation to single process heat sources, and they are not significantly altered by application to process source profiles. Figure 12(a) illustrates the advantage of choosing a working fluid operating near critical conditions on the heat absorption side. Profile 1 (P-R) is well away from critical with the latent heat change much greater than the sensible heating of the liquid. Cycle efficiency is low and hence work output is low. Increasing pressure ratio or changing the working fluid to one which operates nearer critical at the same or similar pressure ratio increases cycle efficiency by raising the top-cycle temperature, illustrated by profile 2 (P-S). Choosing a supercritical profile such as 3 (P-T) clearly maximizes cycle efficiency, because it maximizes upper-cycle temperature. Figure 12(b) illustrates the load vs. level tradeoff. Profile 1 (which might be fluorocarbon) can absorb more heat than profile 2 (which might be steam), but only at a lower level. Use of the process source profile allows the designer quickly to identify obvious alternatives.

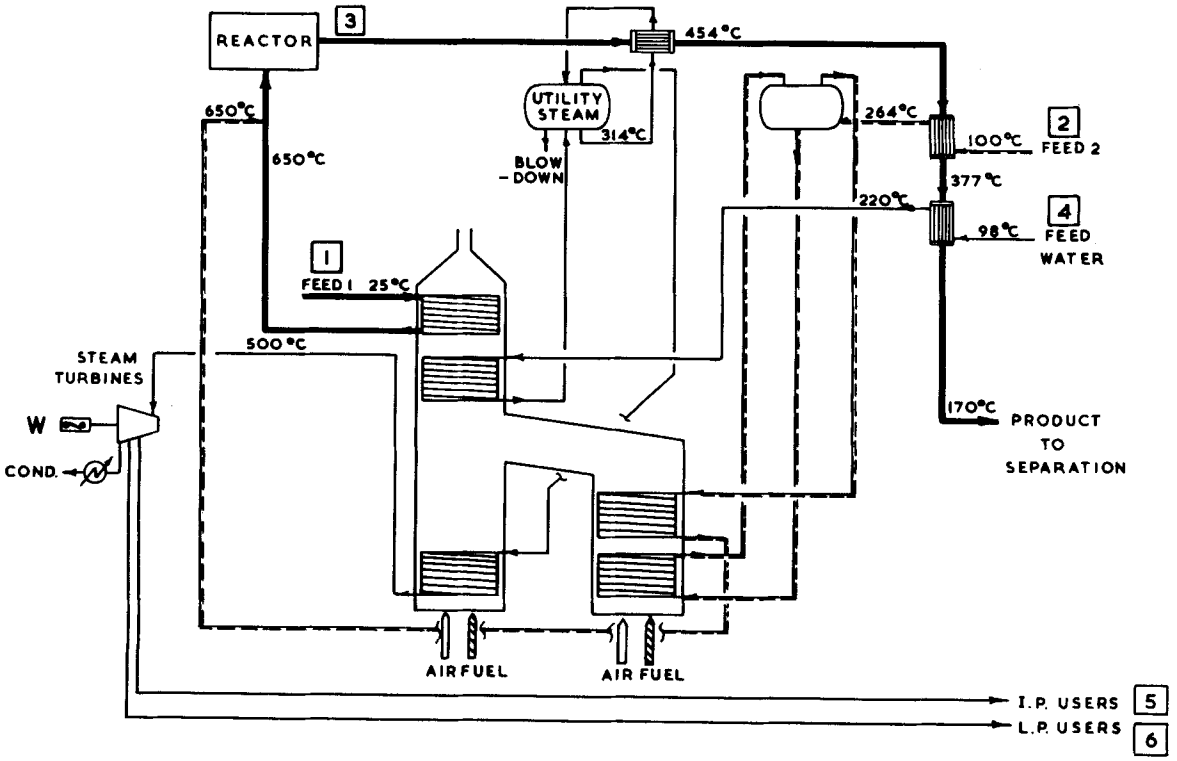

Figure 13. Simplified case study flowsheet.

TABLE 1. CASE STUDY PROBLEM DATA

Stream Number and Type	Supply Temp. (°C)	Target Temp. (°C)	Enthalpy Data Temp. (°C)	Enthalpy (MW)
			Reactor Exit	143.8
			650	97.6
			550	75.1
			450	53.7
3 (Hot)	650	170	350	33.5
			260	16.3
			170	0.0
			100	0.0
			264	15.6
			264	50.4
2 (Cold)	100	650	300	53.2
			350	56.2
			400	58.9
			650	71.4
			25	0.0
			155	14.9
			200	28.4
1 (Cold)	25	650	300	42.6
			400	57.3
			500	72.7
			650	96.0
5 (Cold)	210	210	210	0.0
			210	10.35
6 (Cold)	140	140	140	0.0
			140	48.08

Power Requirement = 65 MW

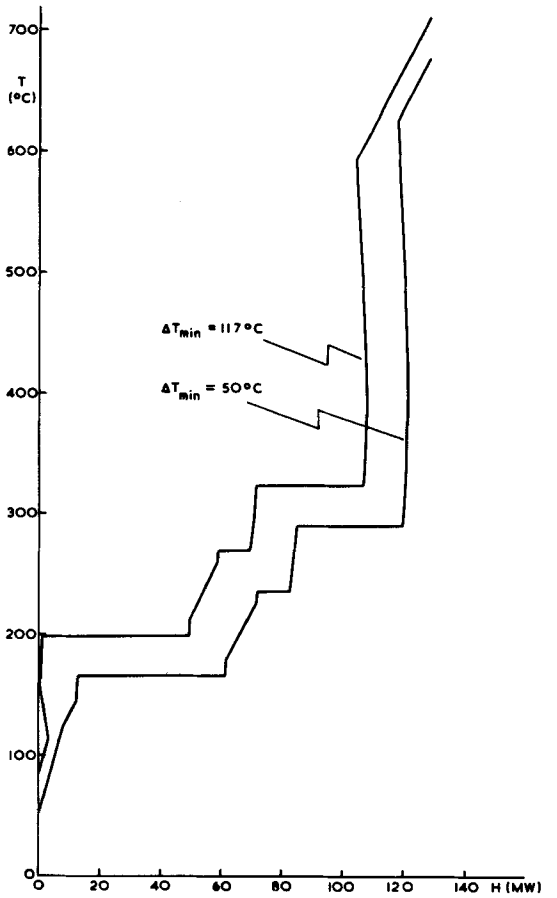

Figure 14. Case study source/sink profiles.

CASE STUDY

A case study will now be introduced to illustrate the use of the process source/sink profile in the context of design. The data are derived from a development study performed in ICI on a "tonnage" chemical process.

The Problem

Figure 13 shows a simplified flowsheet of the "front end" of the process. For the purposes of direct process heat integration, the front end and separation end of the process are separate. However, 19.6 T/h of 19-bar (1.9-MPa) steam and 80.7 T/h of 3.6-bar (360-kPa) steam are provided by the front end for use in separation duties. Also the front end is required to produce 65 MW of shaft power for process use. The problem is to design a heat and power system which meets these requirements as well as the process conditions of the front end itself.

The system as shown represents "state-of-the-art" design. The power is produced by a steam Rankine cycle, which takes heat both from the process (hot reactor effluent) and from a fired heater. To evaluate the design, the working fluid streams must be identified and eliminated from the process stream system. In Figure 13, stream 1 (first process feed), stream 2 (second process feed, which ultimately mixes with first-process feed), and stream 3 (reactor effluent) constitute the front-end process stream set. Stream 4 only transfers heat to the power system and so is not included in the analysis. The steam supplies to the separation end must be included as *cold* process streams (No. 5 and No. 6), because they represent a service duty on the front end.

The temperature–enthalpy data for the process streams are given in Table 1. For good control and process design reasons, stream 3 must be exchanged against steam-raising or other evaporation duty to about 650°C. Hence in a design incorporating a steam turbine, the heat available in stream 3 above 650°C is logically added to the power cycle so that it can be converted to power at 100% efficiency. In a design incorporating a gas turbine only, this heat could be matched either against raising the IP and LP steam required by the separation end, or against stream 2 vaporization with the surplus going to, say, LP raising. This choice will be considered later when the gas turbine scheme is discussed.

The design shown in Figure 13 requires 232 MW of utility heating. (See Appendix.)

Choice of ΔT_{min}

The choice of ΔT_{min} values at this stage of the study warrants some discussion. In heat recovery problems having a pinch, the utility requirements are always sensitive to the choice of ΔT_{min} (Linnhoff et al., 1979). Further, for *any* heat recovery problem, the choice of ΔT_{min} affects the shape of the process source/sink profile. The case study data, when analyzed by the Problem Table method, show "threshold" behavior, i.e., only hot utility is required for values of ΔT_{min} less than 117°C (Linnhoff and Hindmarsh, 1982). However, Figure 14 shows profiles plotted for ΔT_{min} values of 117 and 50°C. It can be seen that although the total size of the heat sink is not changed, the profiles are quite different, in level *and* in shape. Therefore, when matching heat engines against processes, the choice of ΔT_{min} can affect the energy performance of the total system significantly.

Finding the correct economic values for process/process and heat engine/process, ΔT_{min} is a rather complex procedure involving optimization and is currently under research. Fortunately, it is not necessary to consider such optimization during the early stages of a study. The practical heat engines available to the chemical process design engineer are few in number, very different in kind, and generally produce very different results in application on the same process. To select the right type, it is normally sufficient to choose "experience values" for all ΔT_{min}s. In the few cases where there may be doubt, coarse optimization on two systems will be required to make the right choice.

In the present case study, process streams are assigned ΔT_{min}

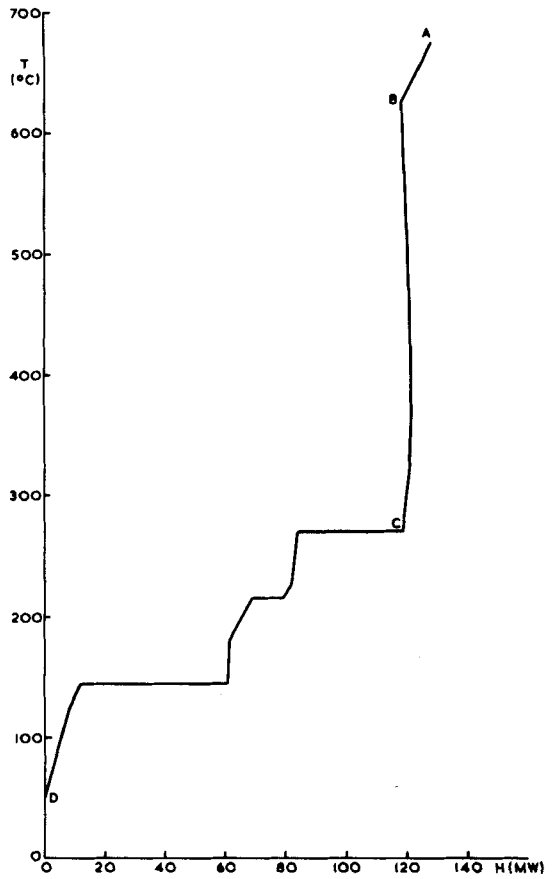

Figure 15. Case study selected source/sink profile.

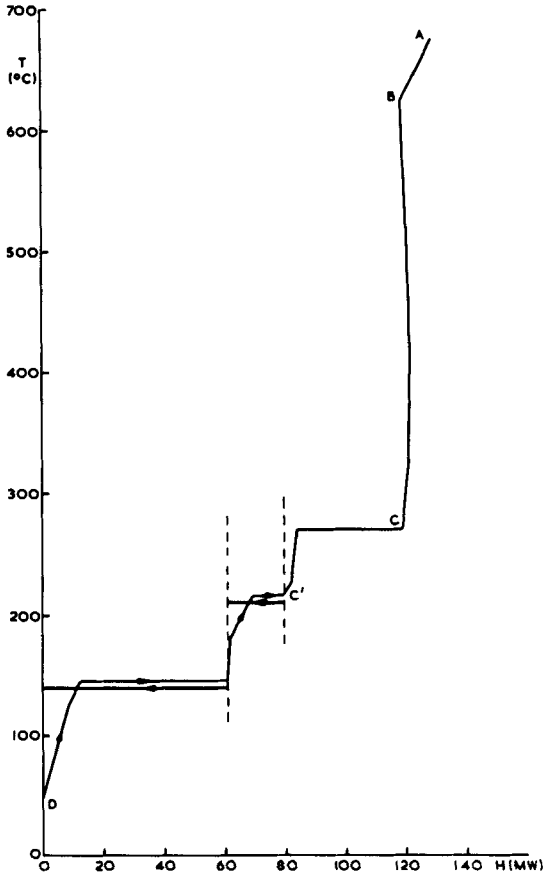

Figure 16. Case study, targeting for steam turbine.

TABLE 2. CASE STUDY HEAT CASCADE FROM PROBLEM TABLE ANALYSIS OF TABLE 1 DATA

Interval Temp. (°C)	Heat Flow (MW)
675	128.23
625	117.96
525	119.93
425	120.93
375	120.98
325	120.73
289	119.70
269	118.78
269	83.98
235	82.41
225	81.85
215	79.71
215	69.36
180	61.87
145	60.87
145	12.79
125	8.60
50	0

contributions of 25°C except where evaporative changes occur, and then contributions of 5°C are assigned. Based on these values, the process source/sink is shown plotted in Figure 15, from the Problem Table heat flows given in Table 2.

Coarse Analysis

Before performing any further calculations, some important conclusions can be drawn about the total system by inspection of Figure 15. The process is a very large heat sink which extends from high to near-ambient temperature and falls into two distinct regions: a very high temperature region BA, and a low-to-moderate region DC. The temperature of region BA is so high that it cannot be satisfied by exhaust from any practical engine; i.e., it must be supplied by direct heating. This leaves the profile DC for matching with an engine exhaust.

Targeting for a Steam Turbine

Large amounts of IP and LP steam are required by the separation end of the process. This dictates that the steam turbine should produce "back-pressure" steam at these levels. By assigning a ΔT_{min} contribution of −5°C to the back-pressure steam, the result of a "match" between the IP or LP required and IP or LP supplied, Figure 16, is a "ΔT_{min}" of 0°C. In other words, the direct supply of steam for the separation end is represented. The amounts of IP and LP required by the separation end are 10.35 and 48.08 MW, respectively. However, from Figure 16 it is clear that a total of 18.84 MW of IP and 60.87 MW of LP can be supplied to the total process. In other words, the "front end" can absorb about 8.5 MW of IP and about 12.8 MW of LP. Since the front-end process streams in these regions have ΔT_{min} contributions of 25°C, the steam-to-process ΔT_{min} is 20°C.

Certain cycle parameters must be chosen by the designer to calculate the steam turbine power output. Principally, turbine inlet temperature and pressure must be chosen. In this case study, they are fixed at 500°C and 104.5 bar (1,500 psig; 10.45 MPa) both for the "base case" (Figure 13) and in the present targeting exercise. These values are considered to be the practical maxima. Values of other parameters (for example, turbine efficiency) are given in the Appendix. Also given in the Appendix is the assumed steam cycle flowsheet. (Note that, because we are targeting for best energy performance, steam system economizer-interchangers, Figure 10(e), are assumed to be incorporated where thermodynamically possible when full-cycle calculations are performed.)

Having determined the IP and LP steam flows to the process and

having fixed turbine inlet conditions, the next step is to make a quick estimate of the power implications of these back-pressure flows. As shown in the Appendix, the estimate is 23 MW. Since the power required is 65 MW, it is clear that a third steam turbine stage must produce large quantities of power by condensation against cooling water.

A remaining question is whether adding a third back-pressure steam level to supply region C'C (Figure 16) is worthwhile. The total load required by this region is 38.25 MW, and when supplied by back-pressure steam (at a ΔT_{min} of 20°C) yields 2.15 MW of power at 100% efficiency. (See Appendix for calculations.) Since this power would replace 2.15 MW generated at approximately 36% efficiency by the "condensing" steam turbine, the net hot utility saving is 3.8 MW. This saving is very low, considering the cost implications of the extra level (i.e., additional turbo-machinery, steam and condensate handling systems, and heat exchanger transferring 38.25 MW at 20°C ΔT). It can thus be discounted as uneconomic on the basis of this very quick analysis.

The steam turbine design which achieves 65-MW total power output, incorporating a combination of two "back-pressure" stages and a "condensing" stage, is calculated in the Appendix. An economizer–interchanger which exchanges IP steam against boiler feed water down to a ΔT_{min} of 20°C is incorporated, carrying a load of 22.5 MW. This cycle requires a net heat input of 212.0 MW. From Figure 16, it can be seen that over the region C'A (a sink of 48.5 MW) hot utility must be supplied. Because 46.2 MW is supplied to the steam system from the hot end of stream 3 (Table 1), the net hot utility requirement for the total problem incorporating the above power cycle is:

$$212.0 - 46.2 + 48.5 = \underline{214.3 \text{ MW}}$$

Hence, saving over base case = $232.0 - 214.3 = \underline{17.7 \text{ MW}}$

Target Steam Turbine System vs. Base Case

The scope for hot utility saving identified above of 17.7 MW must be considered in the light of the method of external heat supply. In the base case (Figure 13), heat can be supplied from a

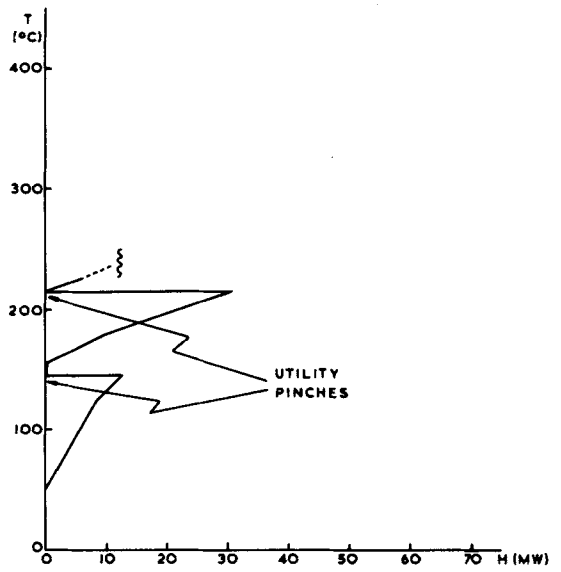

Figure 17. Case study source/sink profile, with addition of steam cycle streams.

furnace with the combustion gases in the convection bank being cooled to the safe limit of 135°C. This corresponds to 95% efficiency. However, Figure 17 shows that this is not possible for the targeted case. By maximizing the use of IP and LP steam, "utility pinches" are created at these levels. Hence, the problem requires only utility heating down to an interval temperature of 215°C. If the heater flue gas itself has a ΔT_{min} contribution of 25°C, it can be cooled only to 240°C against the process. Hence, to achieve a utility heater efficiency approaching 95%, an air preheater would be required.

Note that Figure 17 is derived from a Problem Table analysis which includes the steam-cycle boiler-feed water (a cold stream), and the 22.5 MW of IP steam (a hot stream) consumed in the

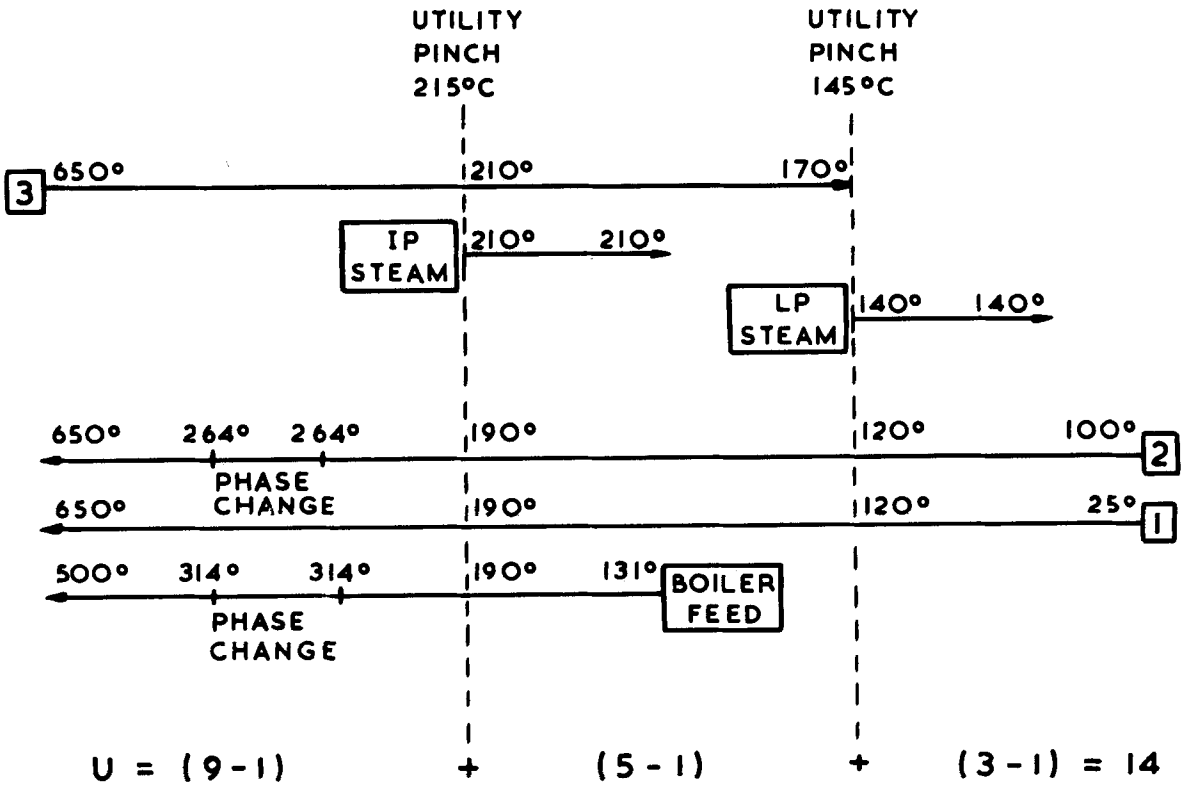

Figure 18. Capital targeting for case study, incorporating steam cycle.

economizer-interchanger. Had the steam cycle not included the economizer, with the steam cycle streams included in the Problem Table analysis, pinches would not have been detected at the IP and LP levels. This simply reflects the fact that available driving forces would not have been fully exploited in the steam-cycle design.

With the inclusion of an air preheater, the efficiency of the fired heater for the targeted case could approach that for the base case. Hence, the net scope for fuel saving is approximately:

$$\frac{17.7}{0.95} = 18.6 \text{ MW}$$

This represents a 7.6% scope for improving the base case design. However, this scope can only be realized at a cost in design complexity.

An indication of this cost can be gained by application of the capital targeting method described by Linnhoff and Hindmarsh (1983). The method involves applying the targeting formula

$$U_{min} = N - 1,$$

where U_{min} = minimum number of heat exchange units, N = number of streams plust utilities, above and below every pinch in the problem, Figure 18. Above the 215° utility pinch, there are four streams plus utility heating. However, stream 2 and the boiler stream must each be regarded as three separate streams, because preheating, evaporation and superheating, cannot be accomplished in one unit. Hence, there are effectively eight streams plus hot utility, making $N = 9$ and hence $U_{min} = 8$. Targeting for the remaining two regions in the problem and adding the totals for all three regions together give the target for the entire problem of 14 units. It should be remembered that outside the context of Figure 18, a match between the hot end of stream 3 and steam raising has already been assumed. However, since the same two streams occur in the hot end of Figure 18, the implied heat load loop can be eliminated by simple merging, and the assumed unit need not be added to the total. On the other hand, it should be remembered that in the targeted case, the fired heater requires an air preheater, and that an economizer-interchanger and a cooling water condenser have been assumed. Hence on this account, the overall number of units targeted is 17.

The base case design (Figure 13) incorporates no IP or LP heating of the front-end process streams or of the boiler-feed water. Hence, it contains no utility pinches. Applying the units targeting formula to the whole problem, therefore, yields $U_{min} = 8$. With the cooling water condenser, the number of units target is 9 and the design in Figure 13 achieves this target.

The conclusion is that the base case is more or less optimum for a design incorporating steam turbines. To realize the small energy scope of 7.6%, the number of exchangers would have to be almost doubled. Even on the basis of preliminary or outline study as presented here, this can be discarded as unattractive. Thus the procedure described in this paper reveals, with little effort, that the "state-of-the-art" flowsheet is indeed "state-of-the-art," if the power generating technology employed is a steam Rankine cycle.

Targeting for a Gas Turbine

It was noted above that with 100% gas turbine drives, the heat from stream 3 above 650°C could either go to raising IP and LP steam (streams 5 and 6), or to the evaporative change in stream 2 with residual heat going to, say, LP-raising.

Case 1:
IP/LP are raised by quench heat.
Heat required by IP-raising (stream 5) = 10.35 MW
Heat required by LP-raising (stream 6) = 48.08 MW
Heat available from stream 3 above 650°C = 46.2 MW
Hence, assuming stream 5 is completely satisfied, heat requirement remaining in stream 6 = 12.23 MW

Case 2:
Stream 2 vaporization/LP against heat from stream 3
Heat required by stream 2 vaporization = 34.8 MW
Heat required by LP raising (stream 6) = 48.08 MW
Heat available from stream 3 = 46.2 MW
Hence, assuming stream 2 evaporization is completely satisfied, heat requirement remaining in stream 6 = 36.68 MW

The process source/sink profiles for these two cases are shown in Figures 19(a) and (b). The positions of the profiles prior to modification (i.e., as in Figure 15) are shown in dotted line.

Note that in either case, the size of the modified heat sink is 82.0 MW, but that the shape of the profiles between points A and B are

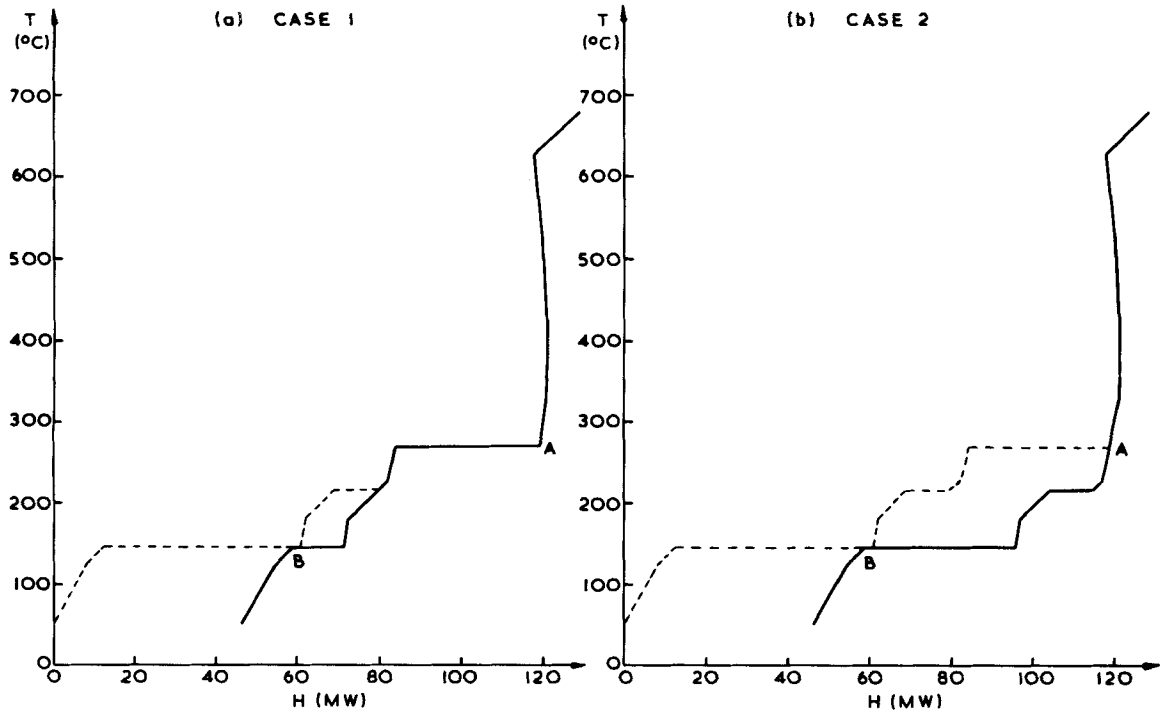

Figure 19. Case study source/sink profiles for gas turbine targeting.

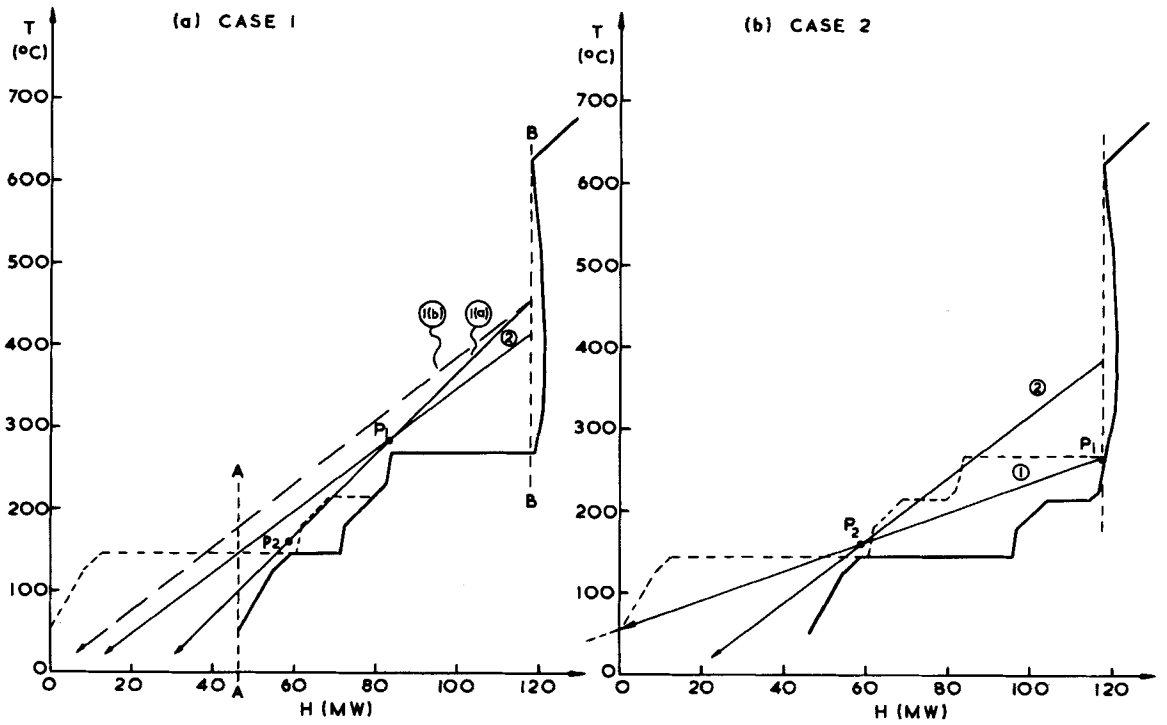

Figure 20. Case study, targeting for gas turbine systems.

different. This influences the target energy performance of the total system.

In targeting for an open-cycle gas turbine, the load vs. level interaction, Figure 9(b), must be considered. A useful concept in exploring the interaction is that of an exhaust "pivot-point." Figure 20(a) illustrates the principle for Case 1. The single exhaust profile which most closely approaches the process sink profile, while supplying the maximum feasible quantity of heat, is profile 1(a). Its points of closest approach to the process profile, assuming a ΔT_{min} contribution assigned to the exhaust of 15°C, are P_1 and P_2. (This means that exhaust-to-process matches have a ΔT_{min} of 40 or 20°C, depending on the stream—see "Choice of ΔT_{min}.") Having constructed profile 1(a), and having defined certain gas turbine cycle parameters (the Appendix), the power output from the cycle with exhaust profile 1(a) can be calculated. The calculation method used for gas turbine cycles is given in the Appendix. In this case, the power output is 50.8 MW, i.e. 14.2 MW short of meeting the plant requirement.

Simply increasing the size of this cycle at constant external exhaust temperature to give the required power output would yield exhaust profile 1(b). This profile nowhere approaches the process sink profile as closely as the ΔT_{min} contribution. This waste of driving force is avoided by exhaust profile 2 which provides the same power but passes through P_1. It is at a lower temperature than profile 1(a) throughout, and so represents a gas-turbine cycle of higher efficiency (for given upper-cycle temperature). This allows a greater amount of heat to be converted into work at 100% net efficiency. The net result is less heat rejected to waste (to the left of A-A in Figure 20(a)). The required power output has been produced by increasing the exhaust flowrate, but with P_1 as "pivot point." In other words, the best cycle has been found by constructing the exhaust profile passing through P_1 and P_2 and by increasing the flowrate with P_1 as pivot to produce 65 MW in the implied gas turbine cycle. The last step requires iterative calculation. However, the iteration is simple, particularly if a programmable calculator is employed.

For exhaust profile 2, the gas turbine cycle requires 167.3-MW heat input and has a cycle efficiency of 38.8% (Appendix).

Exhaust profile matching for Case 2 is shown in Figure 20(b). Comparing Figures 20(a) and (b), P_2 remains in the same position, but P_1 changes position due to the changed shape of the process sink profile. This means that in Figure 20(b), exhaust profile 1 which passes through P_1 and P_2 has a much greater flowrate than profile 1(a) in Figure 20(a). Hence, it implies a power output greatly in excess of plant requirement and at the same time much heated wasted to ambient. Thus, profile 2 is found by reducing the flowrate with P_2 as pivot, until the power output is 65 MW.

In this case for profile 2, the gas turbine cycle requires 160.2-MW heat input and has a cycle efficiency of 40.6% (Appendix). Hence, Case 2, in which the heat from stream 3 above 650°C is used for the evaporative change on stream 2, yields the superior scheme in the combined heat and power system.

As with the steam turbine solution, the method of external heat supply must be considered when calculating the energy target for the total system. The major source of energy in the total system incorporating a gas turbine, is the gas-turbine combustion chamber. This would operate at very high efficiency in modern systems, say 99%. However, the 10.27 MW of heat required by the process at temperatures hotter than any part of the gas turbine exhaust, must be supplied from an independent fired heater. With the process duty at such high temperature (above 600°C), substantial air preheating would have to be incorporated to give the furnace good efficiency. An economic efficiency for such a system might be about 85%. Hence, the total heat input required is:

$$\frac{160.2}{0.99} + \frac{10.27}{0.85} = 173.9 \text{ MW}$$

Target Gas Turbine System vs. Base Case

The base case requires 232.0 MW of utility heating, which if supplied from a 95% efficient heater, yields a net heat requirement of 244.2 MW. Hence the saving over the base case is 70.3 MW or about 29%; i.e., the heat requirement of the base case exceeds that of the alternative design found here by approximately 40%. Thus, we have a very substantial improvement, firmly establishing the superiority of the gas turbine solution for this process. In fact, appropriate costing methods applied at this stage to both the base case and the gas turbine design showed no capital cost advantage for the base case. This is in keeping with the comment made by Linnhoff and Turner (1980) that improving the energy performance of process networks does not necessarily cost capital.

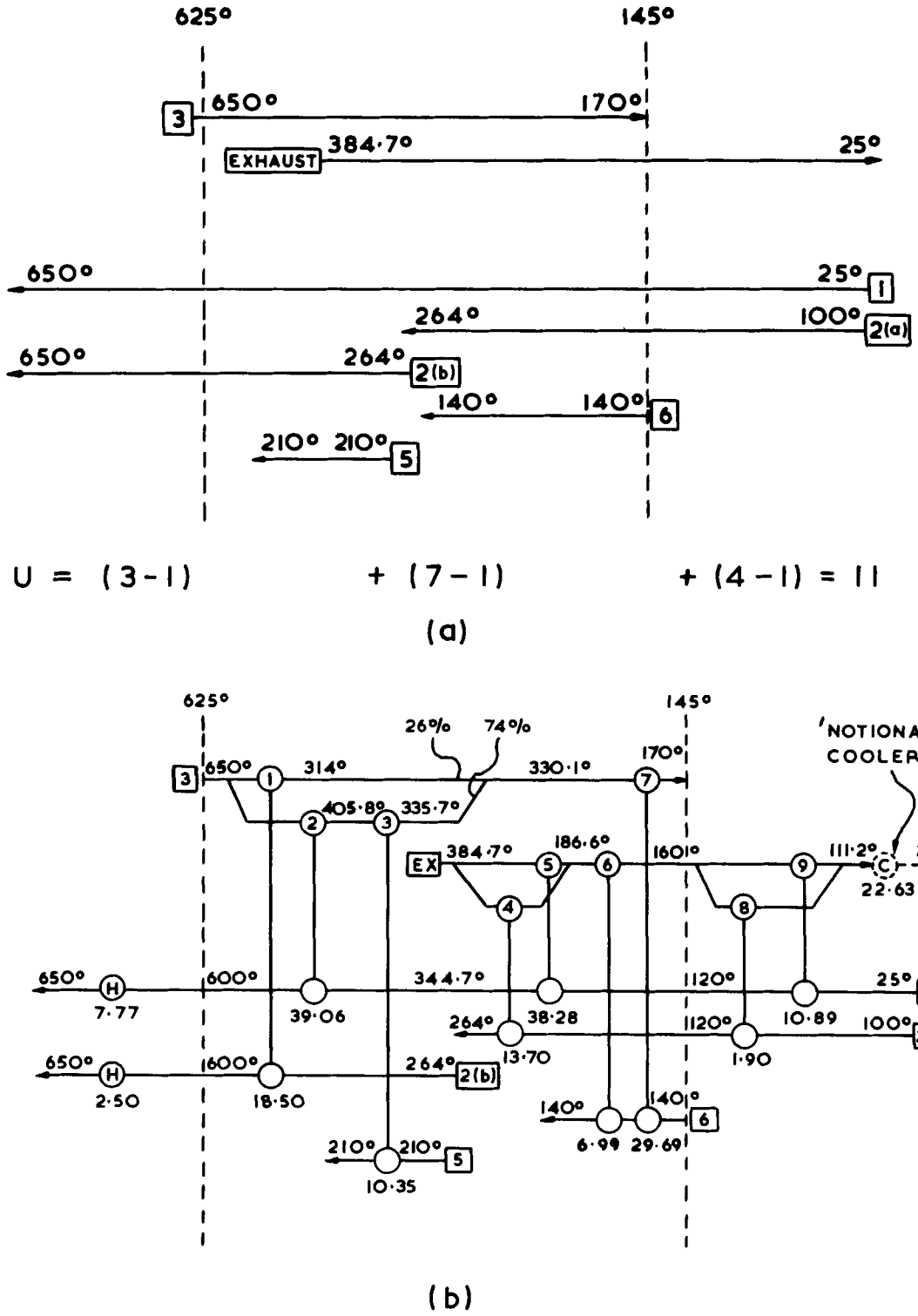

Figure 21. Case study, network design for gas turbine solution.

Note that the position would not be changed materially if the steam cycle had many more levels exhausting to process. It is the irreversibility against the heat source (the steam system accepts heat at 500°C whereas the gas turbine system accepts heat at 1,100°C) that is controlling. For the same reason, the fact that the gas turbine cycle as specified might not be available from a manufacturer, and hence a slightly different cycle might have to be chosen, does not materially affect the comparison.

Heat Exchanger Network Design

As in the steam turbine case, it is possible to target for the number of heat exchange units, Figure 21(a). The stream set (Case 2) comprises the residual parts of streams 2, 3 and 6 (after the assumed matches between the hot end of stream 3 and the evaporative change on stream 2 and part of stream 6, have been allowed for), streams 1 and 5 complete, and the gas turbine exhaust. Pinches occur at 625° and 145°, dividing the problem into three zones. Applying the targeting formula to each zone and summing the results yields a target number of units of 11. Added to this are the assumed matches, i.e., two against the hot end of stream 3, one in the gas turbine itself, and one air preheater. However, the implied cooler on the cold end of the gas turbine exhaust need not be built, since the residual heat in the exhaust simply dissipates in the am-

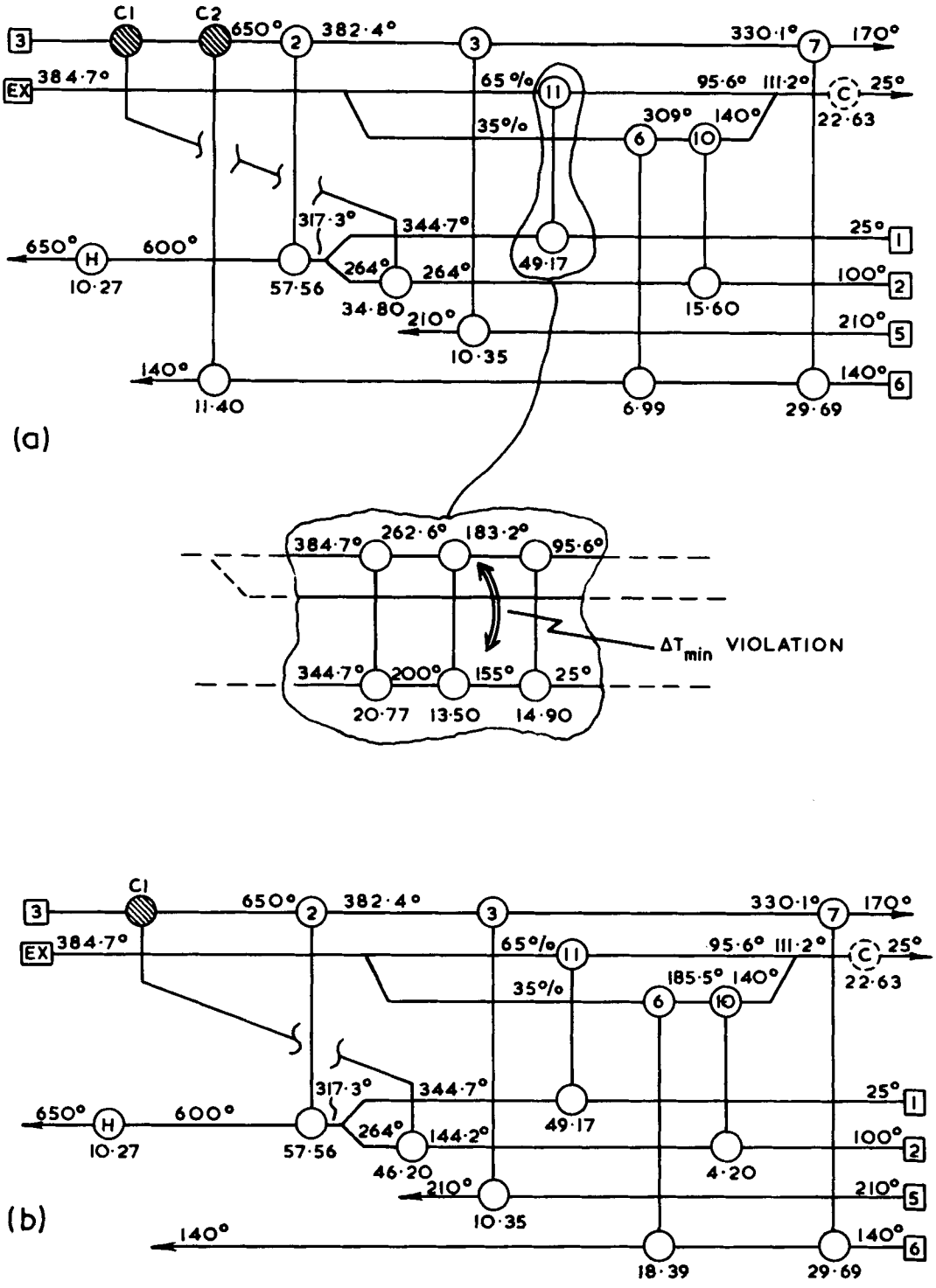

Figure 22. Evolved networks for gas turbine case study solution.

bient air. Hence the target for the entire system is 14. This is still significantly more than for the base case, but at 70-MW energy savings, it might very well be attractive.

A design achieving maximum energy recovery is shown in Figure 21(b). The network is easily arrived at by the "Pinch Design Method" of Linnhoff and Hindmarsh (1982). The hot and cold zones satisfy the units targets. However, the middle zone is one of those unusual systems that cannot be designed with minimum number of units (Linnhoff, 1979), even when stream splitting is employed. One extra unit is required. The full system based on this design would, therefore, incorporate 15 units.

Next, this network is easily simplified by breaking heat load loops at constant network energy performance (Su, 1979; Linnhoff and Hindmarsh, 1982). Figure 22(a) shows four loops broken, and hence four units eliminated. By extending the exhaust stream split across the 145° pinch, and merging match 4 and match 8 into a new match 10, and merging match 5 and match 9 into a new match 11, two units are eliminated. This is possible because the combined heat capacity flowrate of streams 1 and 2 is almost equal to that of the exhaust stream. Match 11 incorporates an internal ΔT_{min} violation due to the nonlinearity of the stream 1 T-H data. This is illustrated in the inset drawing in Figure 22(a). However, over most of the exchanger profile the ΔT is much in excess of ΔT_{min} and the structural simplification gained by the merger is worth the small

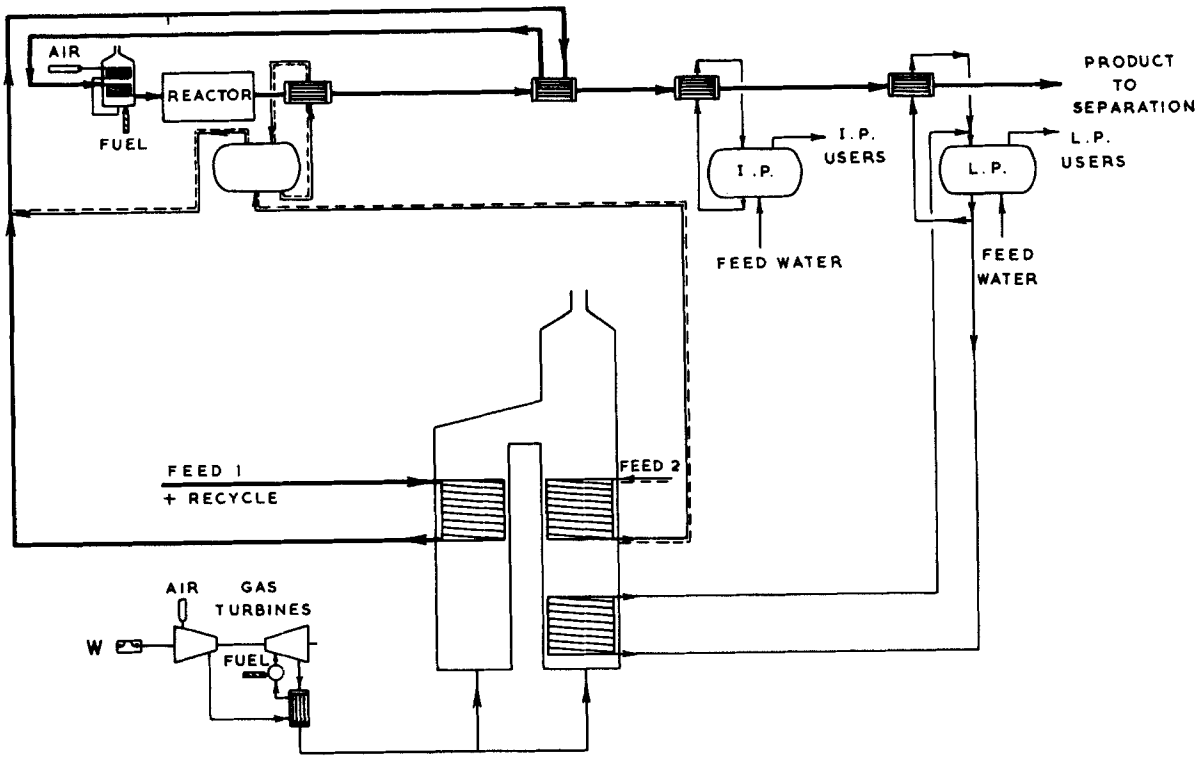

Figure 23. Case study flowsheet for gas turbine solution.

increase in exchanger area. Two further units (a heater and match 1) are easily eliminated by mixing stream 2(b) with stream 1 on the hot side of match 5 (the two mix in the reactor anyway), also saving the stream 3 split. (Note that early mixing would also save one unit in the steam turbine targeting case.)

Figure 22 also shows the "forced" constrained matches, labelled C1 and C2, as required by the energy targeting case 2. Match C2 is seen to be part of a heat-load loop involving matches 6, 10, and C1. This loop is shown broken in Figure 22(b). The effect is to eliminate C2 by requiring C1 partly to preheat the liquid phase of stream 2 as well as to vaporize it. This does not violate the constraint of requiring an evaporative cooling medium for exchange against the hot end of stream 3. If a back-mixed type of unit is employed, all heat transfer to stream 2 in match C1 will be at 264°C.

After these evolutionary steps, the total number of units required for the full system comes down to 10. The flowsheet version of the design is shown in Figure 23.

A Combined Cycle Solution?

The last question to be answered at this (preliminary) stage in

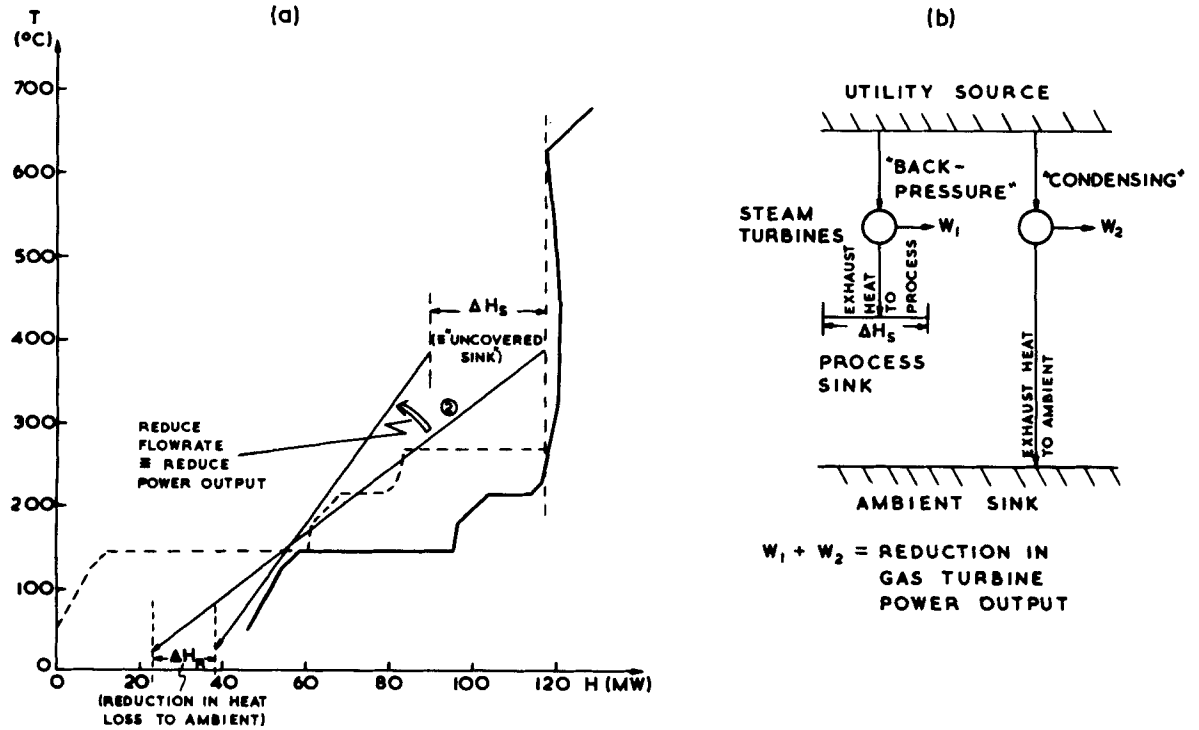

Figure 24. Combined cycle, external steam cycle heat source.

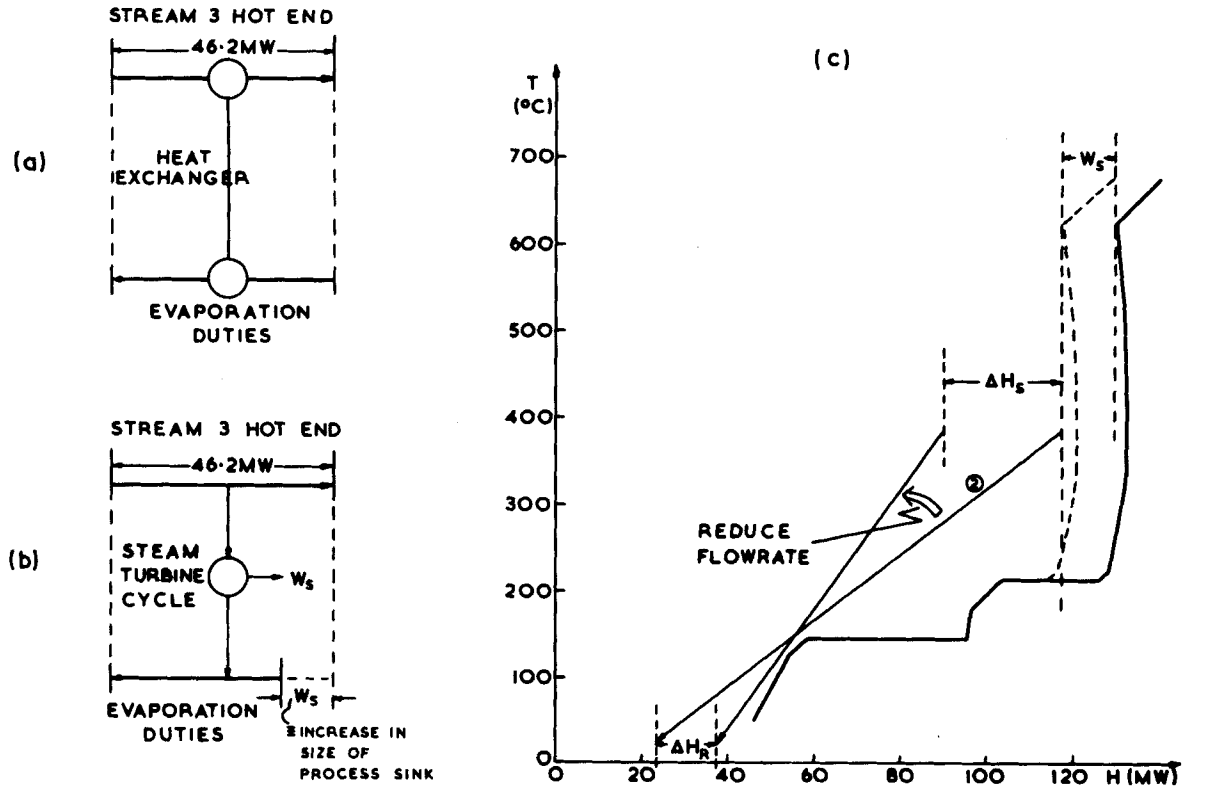

Figure 25. Combined cycle, process steam cycle heat source.

design is whether or not a combined steam turbine/gas turbine solution would produce a significant advantage over the best gas turbine solution.

An obvious way of improving the best gas turbine system is to reduce the exhaust gas flowrate, so that less heat is rejected outside the process sink, Figure 24(a). This then implies reducing the power output of the gas turbine, and replacing the lost power with power from a steam turbine operating at 100% efficiency (i.e., rejecting all its exhaust heat into the "uncovered" process sink), Figure 24(b). If the steam turbine cannot operate at a cycle efficiency high enough to produce all the lost power against the process sink (i.e., in Figure 24(b), $W1$ is less than the lost power), the remaining power must be made up by a "condensing" steam turbine stage rejecting heat to ambient. If this heat rejected to ambient is larger than the reduction in waste heat from the gas turbine (ΔH_R in Figure 24(a)), no net improvement is possible. In the Appendix, it is demonstrated that this is so in the present case study.

The other remaining possibility for improving the gas turbine-based system is to exploit the large temperature difference which exists between the hot end of stream 3 and the evaporative process duties. If a steam turbine cycle were to operate between this source and the process sink, it would produce power at 100% efficiency, Figure 25(a) and (b). The part of the process sink previously satisfied by heat diverted into power would now have to be satisfied directly by utility heating, Figure 25(c). Reducing the size of the gas turbine now unconditionally improves the energy performance of the total system because no heat is rejected to ambient from any other source. Note that the sink "uncovered" by reducing the size of the gas turbine cycle would also be satisfied directly by utility heating, Figure 25(c). It is possible to make a quick "safe-side" estimate of the benefit to be gained, (Appendix). This estimate is 7.4 MW, or 4.3% improvement, which is not large enough to justify the complexity of a combined cycle.

Having explored both single-cycle and combined-cycle configurations, we now have confidence that the proposed solution is the best. No other system based on open gas turbine cycle or steam Rankine cycle technology can give a significantly better performance.

DISCUSSION

The concepts and methods described in this paper share two features in common with the techniques for heat exchanger network design described by Linnhoff et al. in several previous publications. These features are as follows:

Conceptual Understanding vs. Exhaustive Computer Searches

The approach to the synthesis problem is to apply thermodynamics understanding first, before examining the design options. This differs from the more traditional approach to process synthesis problems, where the design task is formulated as a mathematical combinatorial problem from the outset, and computers are used to search through very large solution spaces. By understanding the decomposition between the process source/sink and the power system and by applying engineering knowledge of practical systems, the number of options is reduced dramatically to an extent where they can be examined by hand.

The methods described in this paper certainly could be programmed, but the authors feel that the use of programs should be confined to the repetitive aspects (for example, the power cycle calculations) with the designer remaining in control of the essential profile matching operations. In this way the designer gains a thorough understanding of the tradeoffs in his problem and the options available. This is not to say that at some stage further on in the design task, conventional computer-based modelling and optimization procedures should not be used. They obviously have a role to play. However, the challenge presented today to the design engineer is to keep the computer in its place and to use the most appropriate tool for the task in hand. For preliminary design, that tool is conceptual understanding.

Targeting vs. Design

The method decomposes the problem in a further sense in that it predicts best possible performance prior to detailed design. Again, this is analogous to use of the Problem Table followed by explicit

design methods described by Linnhoff and Flower (Part I), and Linnhoff and Hindmarsh (1983), for heat exchanger networks. This decomposition is a very powerful asset in practical design work. First, it saves time by eliminating early inferior alternatives. Note that we never needed to complete a "design" for the steam turbine-based or combined-cycle solutions. Second, it gives the designer confidence in his flowsheets once the best solution has been found.

ACKNOWLEDGMENT

The authors acknowledge the many contributions of all members of the Process Synthesis team in the ICI New Science Group, and thank ICI Ltd. for permission to publish this paper.

NOTATION

CP = heat capacity—flowrate, MW/°C
H = enthalpy flow, MW
N = number of process streams plus utilities
p = pressure, bar (kPa) a
Q = heat quantity or flow, MJ or MW
R = heat flow rejected by heat engine below the process pinch, MW
S = entropy, kJ/°C
T = temperature, °C
ΔT_{min} = minimum approach temperature difference, °C
U_{min} = minimum number of heat transfer equipment items
W = work or power, MJ or MW
α = heat engine temperature efficiency, dimensionless
η = total heat engine cycle efficiency, dimensionless
η_E = heat engine machine efficiency, dimensionless

Subscripts

IN = input to the process heat recovery problem
OUT = output from the process heat recovery problem

APPENDIX

Case Study Base Case Design

See text, Figure 13 for base case flowsheet. There are five matches against utility heating as follows:

1. Stream 1, 25–650°C,	ΔH = 96.0 MW
2. Stream 2, Evaporation,	ΔH = 34.8 MW
3. Stream 2, 264–650°C	ΔH = 21.0 MW
4. Boiler Feed Water, 220–314°C,	ΔH = 35.1 MW
5. Steam Superheat, 314–500°C,	ΔH = 45.1 MW
Total Utility Heating Required	= 232.0 MW

Steam Rankine Cycle Design for Targeting Case and Base Case

Turbine inlet conditions chosen at 500°C and 104.5 bar (10.45 MPa) a. Assume each stage of the machine has an insentropic efficiency of 85%. Physical properties from steam tables.

Calculate specific enthalpy change across each turbine stage, and define exhaust steam conditions.

From the given stage 1 inlet conditions, h_{IN1} = 3,367 kJ/kg.

Stage 1 outlet is at IP condition (19 bar, 1.9 MPa).

$$\Delta h_{1,ISENTROPIC} = 459 \text{ kJ/kg}$$

$$\Delta h_1 = 0.85 \times 459 \text{ kJ/kg} = 390.2 \text{ kJ/kg}$$

$$\therefore h_{OUT1} = 3367 - 390.2 = 2{,}976.8 \text{ kJ/kg}$$

At p = 19 bar (1.9 MPa), h_{SAT} = 2,798 kJ/kg, Δh_{LATENT} = 1,901 kJ/kg

Hence, calculate desuperheating duty:

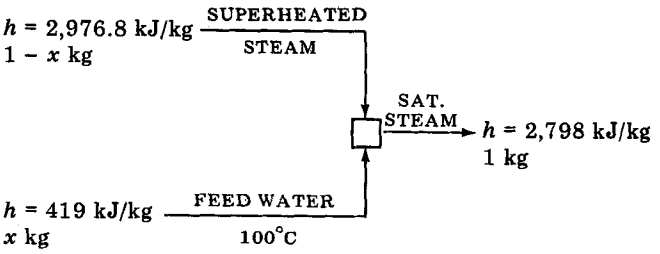

$$x\,(419) + (1 - x)(2{,}976.8) = 2798$$

$$x = \underline{0.06990}$$

Stage 2 inlet = stage 1 outlet

Stage 2 outlet is at LP condition (3.62 bar, 362 kPa)

$$\Delta h_{2,ISENTROPIC} = 339.8 \text{ kJ/kg}$$

$$\Delta h_2 = 0.85 \times 339.8 = 288.8 \text{ kJ/kg}$$

$$\therefore h_{OUT2} = 2{,}976.8 - 288.8 = 2{,}688 \text{ kJ/kg}$$

At p = 3.62 bar, h_{SAT} = 2,734 kJ/kg, Δh_{LATENT} = 2,145 kJ/kg

Hence exhaust is in the wet region.

For 1 kg sat. steam, condensate knock out

$$= \frac{(2{,}734 - 2{,}688)}{(2{,}145 - (2{,}734 - 2{,}688))} = \underline{0.02192}$$

Stage 3 inlet = stage 2 outlet

Stage 3 outlet is at 0.08 bar (8 kPa)

$$\Delta h_{3,ISENTROPIC} = 554 \text{ kJ/kg}$$

$$\Delta h_3 = 0.85 \times 554 = 470.9 \text{ kJ/kg}$$

$$\therefore h_{OUT3} = 2{,}688 - 470.9 = 2{,}217.1 \text{ kJ/kg}$$

At p = 0.08 bar (8 kPa), h_{SAT} = 2,576.4 kJ/kg, Δh_{LATENT} = 2,402.6 kJ/kg

$$\therefore \Delta h_{SUBCOOL} = 2{,}576.4 - 2{,}217.1 = 359.3 \text{ kJ/kg}$$

or a wetness fraction of 15%.

Expansion to 15% wetness is just feasible.

Enthalpy change in the condenser, Δh_{COND} = 2,402.6 − 359.3 = 2,043.4 kJ/kg

Estimate the power available in combination with back pressure flows.

From the targeting procedure,

IP load = 18.84 MW

LP load = 60.87 MW

- Equivalent to IP flow (saturated) = 9.91 kg/s

  LP flow (saturated) = 28.38 kg/s

- Equivalent to IP flow (passout) = 9.91 (1 − 0.0699) = 9.22 kg/s

  LP flow (passout) = 28.38 (1 + 0.02191) = 29.00 kg/s

- Equivalent to stage 1 flow of 38.22 kg/s

  stage 2 flow of 29.00 kg/s

- Equivalent to stage 1 power = $38.22 \times 390.2 \times 10^{-3}$ = 14.91 MW

  stage 2 power = $29.00 \times 288.8 \times 10^{-3}$ = 8.38 MW

  TOTAL = 23.29 MW

Calculate cycle (with economizers) that achieves the requirement of 65 MW. See Appendix Figure A1 for schematic flow diagram of the Rankine cycle. Note that the enthalpy balance around

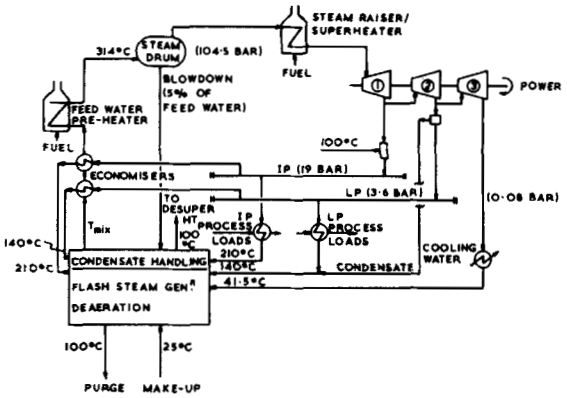

Figure A1. Steam Rankine cycle flow diagram.

the condensate handling system assumes no heat loss to ambient, other than that via the purge flow. It is assumed that the condensate streams are flashed at temperatures high enough to ensure that the temperature of the returning boiler feed water, T_{mix}, can be determined solely by enthalpy balance.

First define flows around the system:

Let the IP steam flow to the IP economizer *prior to desuperheating* be f_1 kg/s.

Let the LP steam flow to the LP economizer *prior to condensate to knockout* be f_2 kg/s.

Hence, power produced via back-pressure routes,

$$W' = 23.29 + 390.2 \times 10^{-3} \times (f_1 + f_2) + 288.8 \times 10^{-3} \times (f_2) \text{ MW}$$

$$\text{Power deficit} = 65 - W' = 41.71 - 0.3902\,(f_1 + f_2) - 0.2888\,(f_2)$$

Extra mass flow required to make up the power deficit,

$$m' = \frac{41.71 - 0.3902\,(f_1 + f_2) - 0.2888\,(f_2)}{(390.2 + 288.8 + 470.9) \times 10^{-3}} \text{ kg/s}$$

$$m' = 36.27 - 0.3393\,(f_1 + f_2) - 0.2512\,(f_2) \text{ kg/s}$$

Desuperheating flow

$$d = 9.91 \times 0.0699 + (f_1) \times \frac{0.0699}{(1 - 0.0699)}$$

$$d = 0.693 + 0.07515\,(f_1)$$

Let the total mass flow inlet to the turbines be m kg/s

$$\text{Hence, flow to steam drum} = \frac{m}{0.95} \text{ kg/s}$$

Blowdown flow,

$$b = m \cdot \frac{(0.05)}{(0.95)} \text{ kg/s}$$

Assuming that the blowdown is flashed to 100°C, enthalpy change of blowdown in cooling to 100°C

$$= m \cdot \frac{(0.05)}{(0.95)} (1{,}427 - 419) \text{ kW}$$

. . . since h_{LIQUID} at 314°C = 1,427 kJ/kg

h_{LIQUID} at 100°C = 419 kJ/kg

and since Δh_{LATENT} at 100°C = 2,257 kJ/kg

$$\text{Flash steam flow} = m \frac{(0.05)}{(0.95)} \frac{(1{,}427 - 419)}{(2257)} \text{ kg/s}$$

$$\text{Purge flow} = m \frac{(0.05)}{(0.95)} \left[1 - \frac{(1{,}427 - 419)}{(2{,}257)}\right] \text{ kg/s}$$

i.e., Purge flow,

$$p_f = 0.02913\,(\text{m}) \text{ kg/s} = \text{make-up flow}$$

Now perform mass balance around condensate handling system:

$$\frac{m}{0.95} = (9.91 + 29.00) + \frac{f_1}{(1 - 0.0699)} + f_2 + m' + b - d$$

After simplification, this yields:

$$m = 74.50 + 0.6607\,(f_1) + 0.4096\,(f_2) \qquad \text{(A1)}$$

Note that a mass balance performed around the turbine set yields the identical equation.

Perform enthalpy balance around condensate handling:

h_{LIQUID} at 314°C = 1,427 kJ/kg

h_{LIQUID} at 210°C = 897 kJ/kg

h_{LIQUID} at140°C = 588.9 kJ/kg

h_{LIQUID} at 100°C = 419.1 kJ/kg

h_{LIQUID} at 41.5°C = 173.8 kJ/kg

h_{LIQUID} at 25°C = 104.8 kJ/kg

Let h_{mix} be the liquid enthalpy of the returning boiler feed water.

Hence,

$$h_{\text{mix}} \times \frac{m}{0.95} = \left[9.91 + \frac{f_1}{(1 - 0.0699)}\right] \times 897 + (29.00 + f_2) \times 588.9 + m' \times 173.8 + b \times 1{,}427 + p_f(104.8 - 419.1) - d \times 419.1$$

After simplification, this yields:

$$m\left(\frac{h_{\text{mix}}}{0.95} - 65.93\right) = 3.199 \times 10^4 + 873.9\,(f_1) + 486.3\,(f_2) \qquad \text{(A2)}$$

Perform enthalpy balances around the two economizers (ΔT_{min} in both of 20°C):

h_{LIQUID} at 190°C = 807.4 kJ/kg

h_{LIQUID} at 120°C = 504.1 kJ/kg

So for the IP economizer,

$$\frac{m}{0.95}(807.4 - 504.1) = \frac{1{,}901\,(f_1)}{(1 - 0.0699)} \qquad \text{(A3)}$$

And for the LP economizer,

$$\frac{m}{0.95}(504.1 - h_{\text{mix}}) = \frac{2{,}145\,(f_2)}{(1 + 0.02192)} \qquad \text{(A4)}$$

These are four equations in four unknowns which can be solved by simple substitution. After such substitution,

$$f_1 = 12.84 \text{ kg/s}, f_2 = -1.94 \text{ kg/s}$$

The negative value for f_2 indicates that T_{mix} is greater than 120°C; i.e., the LP economizer is not feasible.

Hence, set $f_2 = 0$, and reformulate equations:

$$m = 74.50 + 0.6607\,(f_1) \qquad \text{(A5)}$$

$$m\left(\frac{h_{\text{mix}}}{0.95} - 65.93\right) = 3.199 \times 10^4 + 873.9\,(f_1) \qquad \text{(A6)}$$

$$\frac{m}{0.95}(807.4 - h_{\text{mix}}) = \frac{1{,}901\,(f_1)}{(1 - 0.0699)} \qquad \text{(A7)}$$

Simultaneous solution of A5–A7 yields:

$$m = 81.77 \text{ kg/s}$$

$$f_1 = 11.01 \text{ kg/s}$$

$$h_{\text{mix}} = 546.0 \text{ kJ/kg}$$

from which

$$T_{mix} = 130.0°C$$

Hence, heat load on economizer

$$= \frac{1{,}901 \times 11.01 \times 10^{-3}}{1 - 0.0699} = 22.50 \text{ MW}$$

Heat input to cycle

$$= \frac{81.77\,(1{,}427 - 807.4)}{0.95} \times 10^{-3} + 81.77\,(3{,}367 - 1{,}427) \times 10^{-3}$$

$$= 211.96 \text{ MW}$$

This value can be cross-checked by summation of all energy outputs:

Power	65.00 MW
Steam to Process	79.73 MW
Purge	0.75 MW
Condenser Load	66.48 MW
TOTAL	211.96 MW

Steam Cycle Design for Base Case (No Economizers). In this case, process IP load = 10.35 MW

process LP load = 48.08 MW

equivalent to IP passout flow = 5.06 kg/s

LP passout flow = 22.91 kg/s

Power produced via back-pressure routes,

$$W' = (5.06 + 22.91) \times 390.2 \times 10^{-3} + 22.91 \times 288.8 \times 10^{-3} \text{ MW}$$

$$= 17.53 \text{ MW}$$

Power deficit = 47.47 MW

$$m' = 41.28 \text{ kg/s}$$

$$d = 0.38 \text{ kg/s}$$

$$m = 41.28 + 5.06 + 22.91 = 69.25 \text{ kg/s}$$

$$b = 3.65 \text{ kg/s}$$

$$p_f = 2.02 \text{ kg/s}$$

Enthalpy balance around condensate handling:

$$h_{mix} \times \frac{69.25}{0.95} = 5.44 \times 897 + 22.91 \times 588.9 + 41.28 \times 173.8 + 3.64 \times 1427 + 2.02\,(104.8 - 419.1) - 0.38 \times 419.1$$

$$h_{mix} = 410.9 \text{ kJ/kg}$$

from which $T_{mix} = 98.1°C$
Heat input to cycle

$$= 69.25 \frac{(1{,}427 - 410.9) \times 10^{-3}}{0.95} + 69.25\,(3{,}367 - 1{,}427) \times 10^{-3}$$

$$= 208.4 \text{ MW}$$

Heat input to boiler feed water

$$= 74.07 \text{ MW}$$

Heat input to evaporation (Δh_{LATENT} at 314°C = 1,289 kJ/kg)

$$= 89.26 \text{ MW}$$

Heat input to superheating

$$= 45.07 \text{ MW}$$

Estimate Power Output in Combination with Back-Pressure Level Supplying Latent Heat for Stream 2

Process Duty = 38.25 MW (difference between heat flows at 625°C and 215°C)
Process Temperature = 264°C
Back Pressure Steam Condensing Temperature = 284°C
Condensing Pressure = 68.2 bar (6.82 MPa)

$$\Delta h_{ISENTROPIC} = 132 \text{ kJ/kg}$$

$$\Delta h_{STAGE} = 112.2 \text{ kJ/kg}$$

$$\therefore h_{OUT} = 3{,}254.8 \text{ kJ/kg}$$

Note, at p = 68.2 bar (6.82 MPa), h_{SAT} = 2,774.5 kJ/kg, Δh_{LATENT} = 1,517 kJ/kg hence the outlet steam is considerably superheated.
Steam flow to process, assuming no de-superheating,

$$= \frac{38.25 \times 10^3}{(3{,}254.8 - 2{,}774.5 + 1517)} = 19.15 \text{ kg/s}$$

Power Output = $19.15 \times 112.2 \times 10^{-3} = 2.15$ MW

Gas Turbine Cycle Design for Targeting Cases

Assume a gas turbine cycle with interchanger, as shown in Figure 10(b). The following values of cycle parameters are assumed:

Combustion Chamber Temperature, T_3	= 1,100°C
Ambient Temperature, T_1	= 25°C
Ambient Pressure	= 1.0 bar
Compressor Isentropic Efficiency, η_c	= 0.85
Turbine Isentropic Efficiency, η_t	= 0.87
Mechanical Transmission Efficiency η_m	= 0.99
Combustion Chamber Pressure Loss, Δp_b	= 5%
Heat Exchanger Air-Side Pressure Loss, $\Delta p_{g(H)}$	= 3%
Heat Exchanger Exhaust-Side Pressure Loss, $\Delta p_{a(H)}$	= 0.04 bar (4 kPa)
Heat Exchanger ΔT_{min}	= 40°C
Mass Flow Ratio, Exhaust to Air, m_g/m_a	= 1.0137

Note, calculation of m_g/m_a should be iterative, involving repeated cycle calculation. However, the calculations are insensitive to the value of m_g/m_a. The above value was calculated assuming methane as fuel and a net cycle efficiency of 35%.

Cycle Calculation Method. For exhaust profiles identified by the main text procedure, Figures 20(a) and (b), the following cycle calculation procedure is employed.

Identify the exhaust heat capacity flow rate by construction:

i.e., $CP = m_g \cdot \overline{Cp}_{g(E)}$ MW/°C

where m_g = exhaust mass flowrate, T/s

$\overline{Cp}_{g(E)}$ = mean value of exhaust gas heat capacity, over T_6 to T_1

Knowing $\overline{Cp}_{g(E)}$ from physical properties, calculate m_g.

Identify T_6 from the targeting construction. In the interchanger (internal heat exchanger), ΔT_{min} occurs at the hot end, i.e.

$$T_4 - T_5 = \Delta T_{min}$$

At the cold end,

$$T_6 - T_2 > \Delta T_{min}$$

$$T_2 = T_6 - \Delta T_{min} - \Delta \qquad \text{(B1)}$$

On the first iteration, set $\Delta = 0$. Since T_6 and ΔT_{min} are known, this gives an initial value for T_2.
Over the compressor,

$$T_2 - T_1 = \frac{T_1}{\eta_c}\left[\frac{p_2}{p_i}\frac{\overline{\gamma}_a - 1}{\overline{\gamma}_a} - 1\right] \quad \text{(B2)}$$

Where p_1, p_2 are point stagnation pressure values, $\overline{\gamma}_a$ = mean value of air heat capacity ratio. (Note that value of T_1 should be absolute.) Solving Eq. B2 yields p_2 since all other values are known.

Hence,

$$p_3 = p_2\,(1 - \Delta p_b - \Delta p_{a(H)}) \quad \text{(B3)}$$

and

$$p_4 = p_1 + \Delta p_{g(H)} \quad \text{(B4)}$$

Over the expander,

$$T_3 - T_4 = \eta_t \cdot T_3\left[1 - \left(\frac{p_4}{p_2}\right)\frac{\overline{\gamma}_g - 1}{\overline{\gamma}_g}\right] \quad \text{(B5)}$$

(T_3 should be absolute.) yielding T_4, and hence T_5, since

$$T_5 = T_4 - \Delta T_{\min} \quad \text{(B6)}$$

Air-side specific enthalpy change across the interchanger,

$$\Delta h_{a(H)} = \overline{C}p_{a(H)}(T_5 - T_2)\ \text{kJ/kg} \quad \text{(B7)}$$

Exhaust gas specific enthalpy change across the interchanger,

$$\Delta h_{g(H)} = \frac{\Delta h_{a(H)}}{m_g/m_a} \quad \text{(B8)}$$

and

$$\Delta h_{g(H)} = \overline{C}p_{g(H)}(T_4 - T_6) \quad \text{(B9)}$$

yielding T_6. This value is then compared with the true value, and the difference added to the value of Δ employed in the last iteration (Eq. B1). The calculation sequence is then repeated.

Convergence is obtained very rapidly (to about 1/2 degree after 2 iterations).

After convergence, proceed:

Specific Compressor Work (converted to exhaust basis)

$$W_c = \frac{\overline{C}p_{a(c)}(T_2 - T_1)}{\eta_m \times m_g/m_a}\ \text{kJ/kg} \quad \text{(B10)}$$

Specific Turbine Work $W_t = \overline{C}p_{g(T)}(T_3 - T_4)$ kJ/kg (B11)

Net Specific Work Output $W_s = W_t - W_c$ kJ/kg (B12)

Total Power Output $W = m_g \cdot W_s$ MW (B13)

Net Heat Output $Q = W + m_g \cdot \overline{C}p_{g(E)}(T_6 - T_1)$

$$+ \frac{m_g}{m_g/m_a}\left(\frac{1}{\eta_m} - 1\right)\overline{C}p_{a(c)}(T_2 - T_1)\ \text{MW} \quad \text{(B14)}$$

Also,

$$Q = m_g \cdot \overline{C}p_{g(B)}(T_3 - T_5) \quad \text{(B15)}$$

Normally, using mean values for C_p, Eqs. B14 and B15 do not differ by more than 3%.

Also, Heat Exchanger load, $\Delta H_{(H)} = m_g \cdot \Delta h_{g(H)}$ (B16)

The above simple sequential calculation is readily performed by programmable calculator. The results quoted below were all obtained in this way.

Calculate values for various cycle matches. (See Figure 20).
Case 1: Exhaust profile passes through P_1 and P_2 (profile 1(a)).

P_1 Temperature = 284°C, P_2 Temperature = 160°C,

$$\Delta H,\ P_1 \rightarrow P_2 = 24.99\ \text{MW}$$

$$\therefore m_g\overline{C}p_{g(E)} = \frac{24.99}{284 - 160} = 0.2015\ \text{MW/°C}$$

$$\Delta H,\ P_1 \rightarrow BB = 33.98\ \text{MW}$$

$$\therefore T_6 = 284 + \frac{33.98}{0.2015} = 451.6\text{°C}$$

Employing the following physical properties:

$$\overline{\gamma}_a = 1.378$$

$$\overline{\gamma}_g = 1.321$$

$$\overline{C}p_{g(E)} = 1.051\ \text{kJ/kg} \cdot \text{°C}$$

$$\overline{C}p_{g(T)} = 1.187\ \text{kJ/kg} \cdot \text{°C}$$

$$\overline{C}p_{g(H)} = 1.110\ \text{kJ/kg} \cdot \text{°C}$$

$$\overline{C}p_{a(c)} = 1.030\ \text{kJ/kg} \cdot \text{°C}$$

$$\overline{C}p_{a(H)} = 1.080\ \text{kJ/kg} \cdot \text{°C}$$

The following results are obtained:

$$W = 50.8\ \text{MW},\ Q = 137.7\ \text{MW}$$

$$\text{Cycle Efficiency},\ \eta = 36.9\%$$

Case 1: Profile 2. Find the profile passing through P_1 which implies a cycle producing exactly 65 MW of power.

Guess T_6, giving $m_g \cdot \overline{C}p_{g(E)}$ and hence W. Update T_6 and recalculate.

At the final iteration, using the following physical properties:

$$\overline{\gamma}_a = 1.388$$

$$\overline{\gamma}_g = 1.319$$

$$\overline{C}p_{g(E)} = 1.048\ \text{kJ/kg} \cdot \text{°C}$$

$$\overline{C}p_{g(H)} = 1.192\ \text{kJ/kg} \cdot \text{°C}$$

$$\overline{C}p_{g(H)} = 1.113\ \text{kJ/kg} \cdot \text{°C}$$

$$\overline{C}p_{a(C)} = 1.023\ \text{kJ/kg} \cdot \text{°C}$$

$$\overline{C}p_{a(H)} = 1.082\ \text{kJ/kg} \cdot \text{°C}$$

The following results are obtained:

$$\text{For } T_6 = 414.4\text{°C and } m_g \cdot \overline{C}p_{g(E)} = 0.2606$$

$$W = 65\ \text{MW}$$

$$Q = 167.3\ \text{MW}$$

$$\eta = 38.83\%$$

Pressure Ratio $p_2/p_1 = 11.41$

$$\Delta H_{(H)} = 48.14\ \text{MW}$$

$$m_g = 0.2487\ \text{T/s}$$

Case 2: Profile 1.

$$P_1 \text{ Temperature} = 265\text{°C},\ P_2 \text{ Temperature} = 160\text{°C}$$

$$\Delta H,\ p_1 \rightarrow p_2 = 58.97\ \text{MW}$$

These values, using the Case 1, profile 2 physical properties (for convenience), give the following results:

$$W = 114.9\ \text{MW}$$

$$Q = 250.7\ \text{MW}$$

$$p_2/p_1 = 4.36$$

$$\Delta H_{(H)} = 229.6\ \text{MW}$$

$$m_g = 0.5359\ \text{T/s}$$

i.e., a totally unrealistic cycle producing far too much power!

Case 2: Profile 2. Find the profile passing through P_2 which implies a cycle producing exactly 65 MW of power.

At the final iteration, using the following physical properties:

$$\bar{\gamma}_a = 1.390$$

$$\bar{\gamma}_g = 1.319$$

$$\bar{C}p_{g(E)} = 1.046 \text{ kJ/kg} \cdot °\text{C}$$

$$\bar{C}p_{g(T)} = 1.194 \text{ kJ/kg} \cdot °\text{C}$$

$$\bar{C}p_{g(H)} = 1.113 \text{ kJ/kg} \cdot °\text{C}$$

$$\bar{C}p_{a(C)} = 1.023 \text{ kJ/kg} \cdot °\text{C}$$

$$\bar{C}p_{a(H)} = 1.082 \text{ kJ/kg} \cdot °\text{C}$$

The following results are obtained:

For $T_6 = 384.7°\text{C}$ and $m_g \cdot \bar{C}p_{g(E)} = 0.2624$ MW/°C

$$W = 65 \text{ MW}$$

$$Q = 160.2 \text{ MW}$$

$$\eta = 40.58\%$$

$$p_2/p_1 = 9.54$$

$$\Delta H_{(H)} = 65.30 \text{ MW}$$

$$m_g = 0.2509 \text{ T/s}$$

Analysis of Combined Cycle Solutions

External Heat Source for Steam Cycle. Refer to Figure A2 of the Appendix. Case 2, profile 2 is shown, and any profile x based on the same cycle but of smaller power output is shown. The reduction in heat lost to ambient in going from profile 2, to profile x is ΔH_R, and the process sink "uncovered" is ΔH_s. Note that in going from profile 2 to profile x the pivot point changes from P_2 to P_2'.

Let the cycle efficiency of the gas turbine be η_{GT}, and the total required power output be W. Hence,

$$\text{Heat rejected by gas turbine} = W\left(\frac{1}{\eta_{GT}} - 1\right) \tag{C1}$$

and

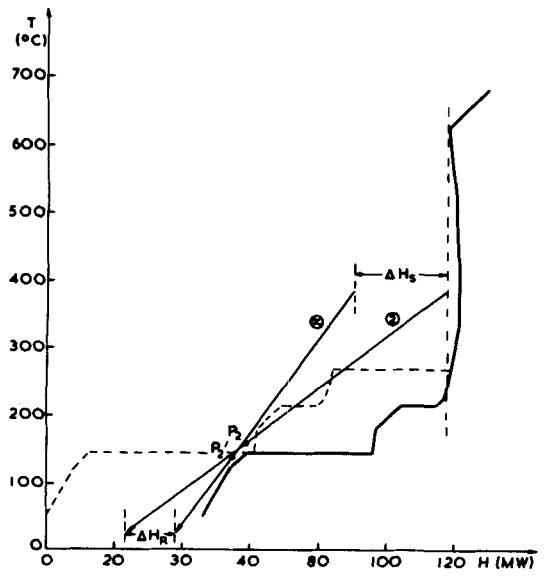

Figure A2. Basis for combined cycle proof.

$$W_x\left(\frac{1}{\eta_{GT}} - 1\right) = W\left(\frac{1}{\eta_{GT}} - 1\right)(\Delta H_S + \Delta H_R) \tag{C2}$$

$$\therefore W_x = W - \frac{(\Delta H_S + \Delta H_R)}{\left(\frac{1}{\eta_{GT}} - 1\right)} \tag{C3}$$

Hence, power deficit caused by reduction in the size of the gas turbine cycle is given by Eq. C3 as

$$\frac{(\Delta H_S + \Delta H_R)}{\left(\frac{1}{\eta_{GT}} - 1\right)}$$

and so this is the total power which must be produced by the steam turbine in the combined cycle solution. Because the cycle efficiency of the steam turbine operating against the process sink (above P_2) is smaller than that of the gas turbine, the power deficit must be made up partly by "back pressure" steam turbine and partly by "condensing" steam turbine.

Let the cycle efficiency of the steam turbine exhausting to process be η_{ST} and that of the steam turbine exhausting to ambient be η'_{ST}. Hence, for the "back pressure" steam turbine, power produced

$$= \frac{\Delta H_S}{\left(\frac{1}{\eta_{ST}} - 1\right)} \tag{C4}$$

power required from "condensing" steam turbine

$$= \frac{(H_S + \Delta H_R)}{\left(\frac{1}{\eta_{GT}} - 1\right)} \frac{-\Delta H_S}{\left(\frac{1}{\eta_{ST}} - 1\right)} \tag{C5}$$

Hence, heat rejected to ambient by the "condensing" steam turbine

$$= \left(\frac{1}{\eta'_{ST}} - 1\right)\left[\frac{(\Delta H_S + \Delta H_R)}{\left(\frac{1}{\eta_{GT}} - 1\right)} \frac{-\Delta H_S}{\left(\frac{1}{\eta_{ST}} - 1\right)}\right] \tag{C6}$$

So for the combined system to produce net energy savings,

$$\Delta H_R > \left(\frac{1}{\eta'_{ST}} - 1\right)\left[\frac{(\Delta H_S + \Delta H_R)}{\left(\frac{1}{\eta_{GT}} - 1\right)} - \frac{\Delta H_S}{\left(\frac{1}{\eta_{ST}} - 1\right)}\right] \tag{C7}$$

For the case study, substitute

$$\eta_{GT} = 0.406$$

$$\eta_{ST} = 0.296 \text{ (See following section.)}$$

$$\eta'_{ST} = 0.360$$

into Eq. C7, yielding

$$\Delta H_R > 0.468\ \Delta H_S + 1.215\ \Delta H_R \tag{C8}$$

Since ΔH_S is positive, L.H.S. ≯ R.H.S. Therefore, savings are not possible.

If a less efficient gas turbine cycle had been chosen with a consequently higher value of T_6, the position is not changed. For example, assume $\eta_{GT} = 0.3375$, $T_6 = 500°\text{C}$. Then for Eq. C7

$$\text{R.H.S.} = 0.158\ \Delta H_S + 0.906\ \Delta H_R$$

But from Figure A2, $\Delta H_S > \Delta H_R$, hence L.H.S. ≯ R.H.S.

Internal Heat Source for Steam Cycle. Assume the steam Rankine cycle absorbs heat from stream 3 above 650°C. To make a "safe-side" estimate of the potential saving, assume the cycle accepts all heat at 324°C, and estimate the Carnot efficiency between this temperature and sink temperature (140°C—L.P. level).

The Carnot efficiency between these temperatures is:

$$1 - \left(\frac{273 + 140}{273 + 314}\right) = 0.296$$

This provides an absolute upper limit to the Rankine cycle efficiency.

Hence, it follows:

Heat Absorbed from Stream 3	= 46.2 MW
Power Produced by Steam Turbine	= 13.7 MW
Required Power Output of Gas Turbine	= 51.3 MW
For the Gas Turbine Cycle Calculated for Case 2,	
Upper Exhaust Temperature T_6 of Figure 10(b)	= 384.7°C
Cycle Efficiency	= 0.4058
For Power Output of 51.3 MW,	
Heat Input to Cycle	= 126.4 MW
Heat Available in Exhaust (0.6 MW Assumed Lost in Transmission)	= 74.5 MW

Making the "best case" assumption that pivot P_2 moves down to 140°C as the exhaust flowrate is reduced:

$$\text{Heat in Exhaust Below } 140°\text{C} = 74.5 \times \frac{(140 - 25)}{(384.7 - 25)}$$

$$= 23.8 \text{ MW}$$

Heat Required by Process Below Equivalent Interval Boundary Temperature = 8.5 MW

$\therefore$ Heat Rejected to Ambient = 23.8 − 8.6 = 15.2 MW

In the Best "Gas Turbine Only" Case, Heat Rejected to Ambient = 22.6 MW

Energy Saved = 22.6 − 15.2 = 7.4 MW

or 4.3% Improvement.

This size of improvement is not large enough to justify the installation of a steam cycle alongside the gas turbine cycle.

LITERATURE CITED

Christodoulou, K., Diploma Thesis, N.T.U., Athens, Greece (1982).

Ichikawa, S., "Use of Fluorocarbon Turbine in Chemical Plants," *Chem. Economy and Eng. Rev.* (Oct., 1970).

Linnhoff, B., "Thermodynamic Analysis in the Design of Process Networks," PhD Thesis, Leeds (1979).

Linnhoff, B., and E. Hindmarsh, "The Pinch Design Method for Heat Exchanger Networks," *Chem. Eng. Sci.* 38, No. 5, 745 (1982).

Linnhoff, B., D. R. Mason, and I. Wardle, "Understanding Heat Exchanger Networks," *Comp. and Chem. Eng.*, 3, No. 1–4, special issue on 214th event of E.F.C.E., Montreux (1979).

Linnhoff, B., and J. A. Turner, "Simple Concepts in Process Synthesis give Energy Savings and Elegant Designs," *Chem. Eng.*, 742 (Dec., 1980).

Sega, K., "Freon Turbine," *Chem. Economy and Eng. Rev.*, 6, 8, 27 (1974).

Stephanopoulous, G., Personal Communication Referring to This Manuscript (1982).

Su, J. L., "A Loop-Breaking Evolutionary Method for the Synthesis of Heat Exchanger Networks," M.S. Thesis, Washington University (1979).

Manuscript received February 25, 1982; revision received October 5, and accepted October 20, 1982.

Studies in Magnetochemical Engineering

Part II: Theoretical Development of a Practical Model for High-Gradient Magnetic Separation

High-gradient magnetic separation (HGMS) is an existing commercial technology which promises to be an effective means for the large-scale separation of both weakly magnetic and practically nonmagnetic, micron-sized particles. It utilizes the strong magnetic forces created typically by placing filamentary ferromagnetic packing materials inside a separator matrix magnetized by a uniform background magnetic field. In this paper, a practical mathematical model for HGMS is developed for quantitatively predicting the grade and recovery of the separated product and the capacity (concentration breakthrough) of the separator. Computer implementation and experimental verification of the new model for HGMS applied to pilot-scale coal beneficiation are described in Part III.

Y. A. LIU

Department of Chemical Engineering
Virginia Polytechnic Institute and State University
Blacksburg, VA 24061

and

M. J. OAK

Department of Chemical Engineering
Auburn University
Auburn University, AL 36849

SCOPE

HGMS is an existing commercial technology which has extended the applicability of magnetic methods from separating the small class of strongly magnetic (ferromagnetic) materials to the much larger class of very weakly magnetic (weakly paramagnetic) materials. The technology is also applicable to separating nonmagnetic (diamagnetic) materials which can be made to associate with magnetic seeding materials. It was developed around 1969 for the wet separation of the weakly

Part I of this series appeared in *Fuel*, 58, 245 (1979).

Correspondence concerning this paper should be addressed to Y. A. Liu. M. J. Oak is with the Department of Chemical Engineering, Princeton University, Princeton, NJ 08544.